Journal of Controlled Release 332 (2021) 312–336

Contents lists available at ScienceDirect

Journal of Controlled Release

journal homepage: www.elsevier.com/locate/jconrel

Review article

Polymeric micelles in drug delivery: An insight of the techniques for their characterization and assessment in biorelevant conditions

M. Ghezzi [a], S. Pescina [a], C. Padula [a], P. Santi [a], E. Del Favero [b], L. Cantù [b], S. Nicoli [a,*]

[a] ADDRes Lab, Department of Food and Drug, University of Parma, Parco Area delle Scienze 27/A, 43124 Parma, Italy
[b] Department of Medical Biotechnologies and Translational Medicine, LITA, University of Milan, Segrate, Italy

ARTICLE INFO

Keywords:
Polymeric micelles
Characterization
Kinetic stability
Drug delivery
Drug release
Biorelevant conditions

ABSTRACT

Polymeric micelles, *i.e.* aggregation colloids formed in solution by self-assembling of amphiphilic polymers, represent an innovative tool to overcome several issues related to drug administration, from the low water-solubility to the poor drug permeability across biological barriers. With respect to other nanocarriers, polymeric micelles generally display smaller size, easier preparation and sterilization processes, and good solubilization properties, unfortunately associated with a lower stability in biological fluids and a more complicated characterization. Particularly challenging is the study of their interaction with the biological environment, essential to predict the real *in vivo* behavior after administration. In this review, after a general presentation on micelles features and properties, different characterization techniques are discussed, from the ones used for the determination of micelles basic characteristics (critical micellar concentration, size, surface charge, morphology) to the more complex approaches used to figure out micelles kinetic stability, drug release and behavior in the presence of biological substrates (fluids, cells and tissues). The techniques presented (such as dynamic light scattering, AFM, cryo-TEM, X-ray scattering, FRET, symmetrical flow field-flow fractionation (AF4) and density ultracentrifugation), each one with their own advantages and limitations, can be combined to achieve a deeper comprehension of polymeric micelles *in vivo* behavior. The set-up and validation of adequate methods for micelles description represent the essential starting point for their development and clinical success.

List of abbreviations

AAmBzA	4-acrylamido benzoic acid
AF4	asymmetric flow field-flow fractionation
AFM	atomic force microscopy
AFU	alpha-L-fucosidase
BCC	body-centered cubic
BSA	bovine serum albumin
BuMA	n-butyl methacrylate
BzMA	benzyl methacrylate
$C_{12}N_4N$	N-dodecyl-1, 4-diaminobutane
Cl	ε-caprolactone
CMC	critical micellar concentration
Cryo-TEM	cryo-transmission electron microscopy
CTAB	hexadecyltrimethylammonium bromide
Cy3	cyanine 3
Cy5	cyanine 5
Cy5.5	cyanine 5.5
Cy7	cyanine 7
Cy5.5-NHS	cyanine 5.5 N-hydroxysuccinimide ester
DAF	5-dodecanoylaminofluorescein
DiI	1,1'-dioctadecyl-3,3,3',3'-tetramethylindocarbocyanine perchlorate
DiO	3,3′-Dioctadecyloxacarbocyanine perchlorate
DL	Drug Loading
DLS	dynamic light scattering
DMA	N,N-dimethylacrylamide
DMF	dimethylformamide
DPH	1,6-diphenyl-1,3,5-hexatriene
EE	Encapsulation Efficiency
F127DA	Pluronic®F127 modified with acrylate end groups
FASSGF	fasted state simulated gastric fluid
FASSIF	fasted state simulated intestinal fluid
FBS	fetal bovine serum
FCC	face-centered cubic
FITC	fluorescein isothiocyanate isomer I
FRET	Foerster resonance energy transfer

(continued on next column)

(continued)

(continued on next page)

* Corresponding author: Advanced Drug Delivery Research Lab) Department of Food and Drug, University of Parma, Parco Area delle Scienze, 27/A, 43124 Parma, Italy.
E-mail address: sara.nicoli@unipr.it (S. Nicoli).

https://doi.org/10.1016/j.jconrel.2021.02.031
Received 7 January 2021; Received in revised form 23 February 2021; Accepted 25 February 2021
Available online 27 February 2021

(*continued*)

GSH	glutathione
HA-ss-DOCA	redox-sensitive hyaluronic acid-deoxycholic acid micelles
HEPES	4-(2-hydroxyethyl)-1-piperazineethanesulfonic acid buffer
HepG2	human liver cancer cells
IgG	immunoglobulin G
i.v.	intravenous
LNCaP	human prostate cancer cells
M109	mouse lung cancer cells
MCCs	multilayered cell cultures
MCF-7	human breast cancer cells
MDR	multi drug resistance
MePEG-*b*-PBTMC	polyethylene glycol)-b-poly (5-benzyloxy-trimethylene carbonate
mPEG	methoxy-polyethylene glycol
mPEG-PCL	methoxypoly(ethylene glycol)-poly(ε-caprolactone)
mPEG-(Cys)4-PDLLA	methoxypoly(ethylene glycol)-(cysteine)4-poly(d,l-lactic acid)
mPEG-PDLLA	methoxypoly(ethylene glycol)- poly(d,l-lactic acid)
MW	molecular weight
MWCO	molecular weight cut-off
NHS	N-hydroxysuccinimide
NP	nanoparticle
NR	nile red
PBS	phosphate buffer saline
PBuOX	poly(2-n-butyl-2-oxazoline)
PCL-PEG-PCL	poly(epsilon-caprolactone)-*b*-poly(ethylene glycol)-poly (epsilon-caprolactone)
PDI	polydispersity index
PDMAEMA	poly(2-(N,N-dimethylamino)ethyl methacrylate)
$PDMAEMA_{co}$	poly(2-(N,N-dimethylamino)ethyl methacrylate)$_x$-block-poly(caprolactone)-block-poly(2-(N,N-dimethylamino) ethyl methacrylate)$_x$,
PEG	polyethylene glycole
PEG-*b*-PCL	poly(ethylene glycol)-block-poly(ε-caprolactone)
PEG-b-PEYM	poly(ethylene glycol)-block-polymethacrylate
PEG-*b*-PLA	poly(ethylene glycol)-block-poly(lactic acid)
PEG-*b*-PLL	poly(ethylene glycol)-block-poly(L-lysine)
PEG-*b*-PPLG	poly(ethylene glycol)-block-poly(γ-propargyl L-glutamate)
PEG-P(Asp(Bzl))	benzyl-esterified poly(ethylene glycol)-block-poly (aspartic acid)
PEG-PDLLA	poly(ethylene glycol)-poly(d,l-lactic acid)
(PEO_{114}-($PDMAEMA_{40}$)$_4$-PEO_{114})	copolymer made of poly(ethylene oxide) and poly (dimethylaminoethyl methacrylate
PLA-*b*-PAA	poly(lactide)-b-poly(acrylic acid)
PLGA	poly-(d,l-lactide-*co*-glycolide) copolymer
PMCL	poly(γ-methyl-ε-caprolactone)
PMGA-g-(PEG/PLA)	heterografted brush copolymer made of poly(glycidyl methacrylate) backbone with PEG and PLA branches
poly(1-O-MAFru)$_{35}$-b-$PMMA_{145}$)	glycopolymer poly(1-O-methacryloyl-β-D-fructopyranose)-block-poly(methyl methacrylate)
poly(PS_{74}-b-DMA_{310})	diblock copolymer of propylene sulfide and N,N-dimethylacrylamide
PPS	poly(propylene sulfide)
PS	propylene sulfide
PS−PI	poly(styrene-*b*-isoprene)
RI	refractive index
SAXS	small angle X-rays
SDS	sodium dodecyl sulfate
SNR	signal-to-noise ratio
SPM	scanning probe microscopy
TEM	transmission electron microscopy
TPGS	D-α-tocopheryl polyethylene glycol 1000 succinate
Tr-SAXS	time-resolved small angle X-rays
Tr-WAXS	time-resolved wide angle X-rays
USAXS	ultrasmall angle X-rays
WAXS	wide angle X-rays
μ-EOC	μ-[poly(ethylethylene)][poly(ethylene oxide)][poly (γ-methyl-ε-caprolactone)]
μ-PEE	μ-poly(ethylethylene)

1. Introduction

Nanomedicine is nowadays one of the most interesting approaches for solving various issues related to drug delivery. Indeed, nanocarriers play a key role in optimizing drug formulation through the improvement of hydrophobic APIs water-solubility [1,2] and the stabilization of easily degradable compounds [3,4]. The great potentialities of nanosystems are the promotion of drug retention in tissues, the protection from enzymatic degradation, the enhancement of cellular uptake, and the highly targeted delivery [5], all aspects having a remarkable impact on the treatments efficacy (Fig. 1A) [6]. Targeted and localized therapies, beneficial also in terms of drug safety profiles, are ensured by exploiting the EPR effect [7] or a controlled drug release triggered either by internal stimuli (biomarker, pH, redox) or by external ones such as temperature, light, radiation, or ultrasounds [8–10]. Besides, nanocarriers are extensively studied as diagnostic agents [11] and theranostic tools, helping to simultaneously diagnose, treat and monitor tumors evolution [6,12]. Finally, the most recent application of nanobased technologies can be found in the delivery of mRNA, as demonstrated by the use of lipid nanoparticles for the administration of the mRNA-based vaccine against SARS-CoV-19 [13–15]. Nanosized systems, depending on the material used for their preparation, can be classified as lipidic, polymeric, inorganic, peptide-based and virus-like nanocarriers (Fig. 1B) [1]. Lipid-based formulations comprise liposomes, rounded-shape self-assembling colloidal structures composed of lipid bilayers surrounding an aqueous core, and solid lipid nanoparticles. Among polymeric nanosystems, formulated by using natural or synthetic polymers, several structures (e.g nanoparticles, nanocapsules, micelles and dendrimers) with different properties can be found while inorganic nanocarriers such as gold nanorods and gold, silica, silver or metal oxide nanoparticles, with the ability of responding to external stimuli, can be used in the field of both imaging and therapy. More details on the materials used, advantages and limitations of nanosystems are summarized in Fig. 1B.

The very high expectations related to nanosystems have not always been met, for a complex series of phenomena, ranging from the potential toxicity of nanomaterials to the low *vivo-vitro* correlation, through the serious difficulties in scaling up the production. Nevertheless, a growing number of nanocarriers is presently approved or in clinical trial [16,17]. Among the nanocarriers, peculiar characteristics are shown by polymeric micelles, self-aggregated colloids made by amphiphilic polymers. These polymers, below a specific concentration, called critical micellar concentration (CMC), are present in solution as single molecules, while above the CMC, they self-assemble into micelles presenting an internal lipophilic core and an external hydrophilic shell (Fig. 2). The consequence is the formation of systems with unique characteristics with respect to other nanocarriers: smaller size enabling the passive targeting to solid tumors (even poorly-permeable ones) [18] and a more efficient cellular internalization [19], good solubilization properties of hydrophobic compounds assimilated in the lipophilic core and a prolonged blood circulation time provided by the naturally present hydrophilic corona [18,20]. Thus, considering their formation by simple self-assembling in solution, micelles are characterized by an easier preparation and a higher scale-up feasibility in comparison to other nanocarriers such as polymeric nanoparticles and liposomes requiring more complex, long lasting and costly manufacturing procedures [19,21].

Additionally, amphiphilic polymers used for micelles preparation can interact with biological membranes and display inherent biological activity: it is well known the inhibitory effect of several polymers on the efflux pumps responsible for MDR in chemotherapy [22,23].

Polymeric micelles for drug delivery have been the subject of intense research, testified by more than 870 papers published in the last 5 years on the use of these nanocarriers for several administration routes[1]. Nevertheless, few clinical trials have been completed or are ongoing, and very little products are approved; additionally, with only one

[1] Source: Scopus, accessed on 29/12/2020; Query Search: TITLE (micelle) AND TITLE-ABS-KEY (polymeric AND micelles) AND TITLE-ABS-KEY (drug AND delivery) AND PUBYEAR > 2015

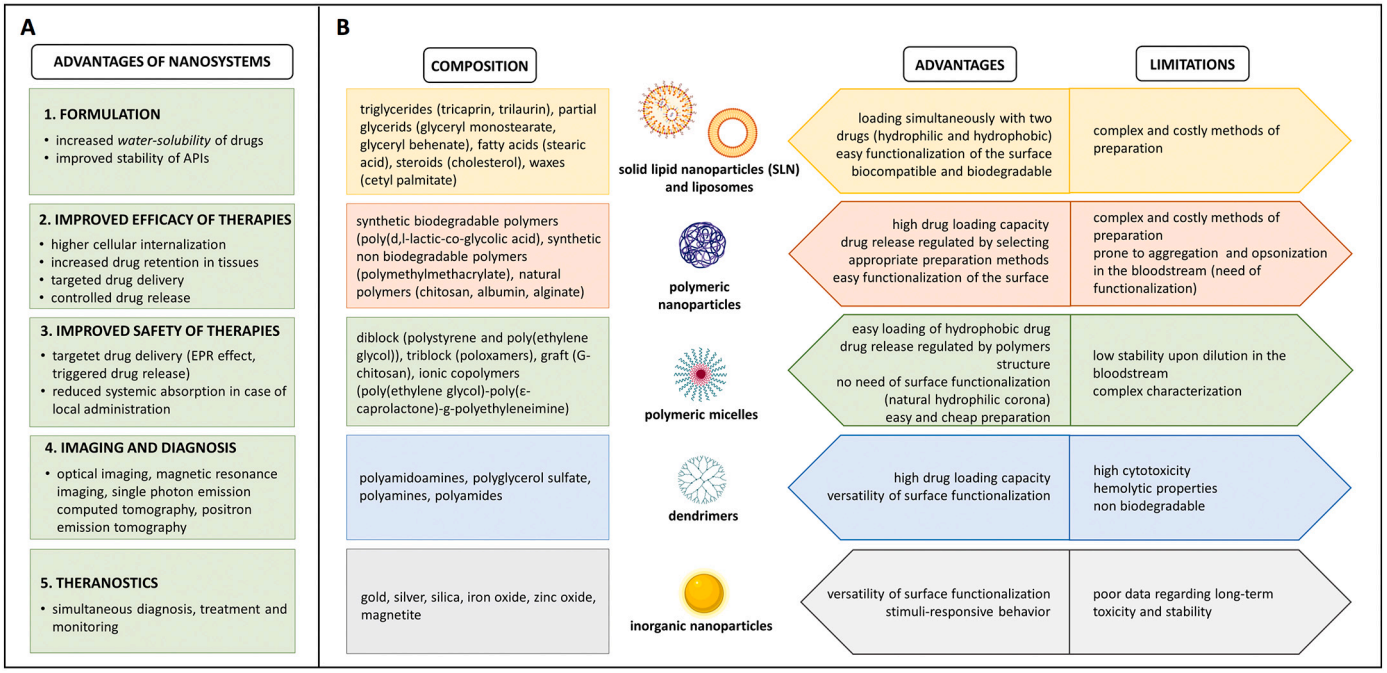

Fig. 1. Panel (A) lists the main advantages of nanosystems in the field of drug delivery. Panel (B) represents in a schematic way the principal types of nanocarriers with regards of their composition (the most common classes of polymers or materials used for their preparation are listed) as well as some hints on their advantages and limitations

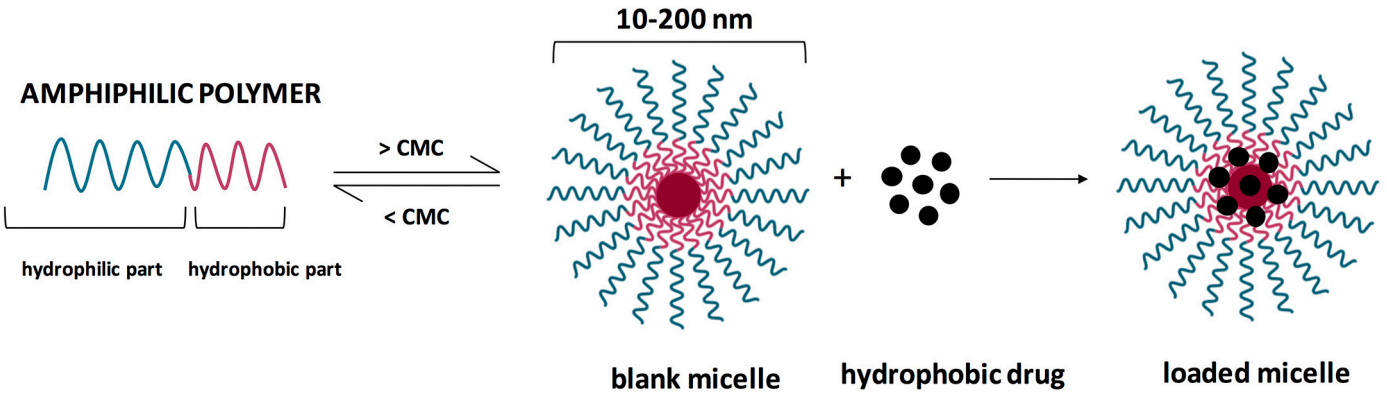

Fig. 2. Schematic representation of polymeric micelles.

exception (a micellar formulation of cyclosporine for ocular application approved by FDA in 2018), all these formulations have been solely developed for the intravenous infusion of chemotherapy drugs [24,25]. As highlighted by Sosnik et Al. in a recent review dealing with challenges toward micelles clinical translation, these carriers, despite their potentiality, still represent a minor contribution in the general nanomedicine field [26], probably because of their lower stability when compared to other polymeric and lipidic nanocarriers. A further problem, linked to their dynamic nature, is represented by the difficulties in their characterization, particularly hard in relation to the study of their interaction with the biological environment. The safety and efficacy of micellar formulations are in relation to their capability to deliver efficiently the active compound to the target site with the highest possible specificity. The in vivo drug delivery from this carrier represents the fundamental step and depends upon several phenomena, particularly complex in the case of association colloids: drug release from intact micelles, micelle's dissociation, interaction with the biological environment, and, in case of intravenous administration, also micelles' distribution and clearance (Fig. 3). These phenomena, in turn, depend upon some basic micelles' characteristics such as size, shape, surface properties, CMC, and kinetic stability. Thus, to shed a light on the potential of these nanocarriers, the definition of these properties, in particular in biorelevant media is essential. Indeed, in 2013, EMA has published a Reflection Paper on block copolymer micelle medicinal products [27]. This paper does acknowledge the complexity of these systems, underlining the need to develop discriminating and biorelevant methods for their characterization.

In this review, after a short description of micelles characteristics, with dutiful citation of the most recent reviews on the topic, several methods and characterization techniques will be presented. Different aspects will be addressed, from the determination of micelles basic characteristics (CMC, size, surface charge, morphology, drug loading, drug release rate) to the more complex methods used to figure out micelles kinetic stability and drug release in biorelevant media, as well as the micelles interaction with biological substrates (cells and tissues).

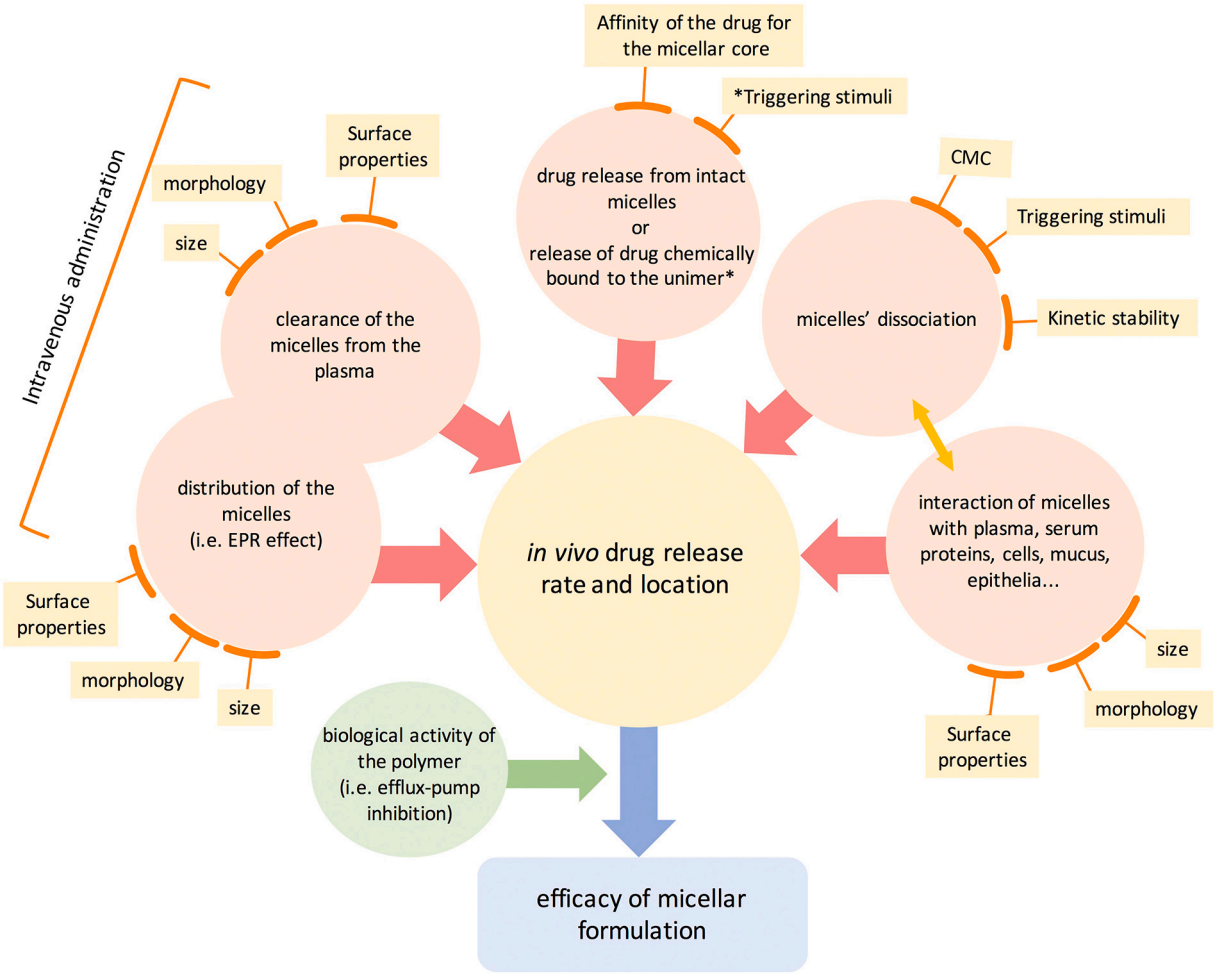

Fig. 3. Schematic representation of the phenomena regulating in vivo drug delivery, in terms of both rate and location, from polymeric micelles. The micelles' properties influencing these phenomena are also illustrated as well as the possible influence of the constituting block-copolymer on the final efficacy

2. Polymeric micelles

2.1. General features

Polymeric micelles are nano-sized drug delivery systems characterized by a core-shell structure originated from self-assembly of amphiphilic block copolymers in aqueous solution (Fig. 2). In diluted aqueous solution, amphiphilic molecules exist separately and amphiphiles work as surfactants reducing the surface tension at the air-water interface. More chains are added to the system, higher is the adsorption at the interface until unimers aggregation occurs due to the saturation of the bulk solution. At this point, Critical Micellar Concentration (CMC) is reached. Thus, the parameter is defined as the minimum concentration of polymers in solution leading to micelles formation. According to this, micelles are stable at concentration of polymeric chains higher than the CMC while disassembling of the system is observed after dilution below the CMC [22,25,28–31]. The CMC value is the most important parameter to define micelles thermodynamic stability. Above the CMC, the equilibrium is dynamic, and characterized by a continuous exchange of the unimers between the micelle and the bulk phase [32]. In addition to thermodynamic stability, another fundamental parameter is the kinetic stability, an index of the micelles tendency to disassembly over time when the system is diluted below the CMC [22].

In comparison with micelles made of low MW surfactants, polymeric micelles' main advantages can be found in their lower CMC and higher kinetic stability. Indeed, for low MW surfactants micelles, disassembling occurs in the range of microseconds whereas polymeric micelles preserve their structure for much longer times. The higher kinetic stability, in addition to lower toxicity, is the reason why polymeric micelles are preferred to low MW surfactants-composed micelles as drug delivery systems [33–35].

The most commonly used polymers for micelles development are amphiphilic di-block copolymers (e.g. polystyrene and poly(ethylene glycol)) and triblock copolymers (e.g. poloxamers) but also graft (e.g. G-chitosan) and ionic (e.g. poly(ethylene glycol)-poly(ε-caprolactone)-g-polyethyleneimine) copolymers are used [28,36–39]. The hydrophilic part is usually composed of PEG (polyethylenglycole), but other polymers are also used such as poly(vinyl pyrrolidone), poly (acryloylmorpholine), or poly(trimethylene carbonate); the hydrophobic segment can be made up of poly(propylene oxide), or polyesters like poly(ε-caprolactone) or polymers and co-polymers of glycolic and lactic acids [36].

Drugs can be encapsulated in the micelles during their formation or in a second step, depending on the method used for the preparation and on the physicochemical characteristics of the drug. The easiest preparation method is the direct dissolution; other methods are dialysis, emulsion with solvent (or co-solvent) evaporation, and solution-casting followed by film hydration. The method selection depends upon both polymer and drug characteristics, and details on this topic can be found in specific reviews [40–43]. Considering that micelles properties such as the polarity and the hydration degree are not uniform within the carrier, the drug can be hosted in different sites, close to the surface or in the inner core, on the basis of its properties [44]. Most of the time, hydrophobic drugs are loaded and hosted in the inner core. In specific cases,

the drug can also be covalently bound to the polymer (polymer-drug conjugate).

2.2. Main properties

The small size, the easy preparation, and the good solubilization properties, make polymeric micelles interesting carriers for different administration routes. They can improve drug bioavailability and produce a controlled and targeted drug release, useful for reducing side effects [45,46]. The most investigated administration route for micelles is the intravenous (i.v.) injection/infusion (mainly exploited for chemotherapy) [18,47–49], but very interesting results in terms of improved drug bioavailability have also been reported following oral [31,50] and topical (ocular, nasal, buccal) [26,36,51,52] administration. As thermodynamically self-assembled systems, micelles are formed by reversible bounds and can be disintegrated by several destabilizing factors. Depending on the administration route, micelles must face different issues: for instance, in the case of i.v. administration, the stress occurring by injection, the high dilution, the presence of serum, and the possible formation of a protein corona. For mucosal and skin delivery, the interaction with mucus and sebum, and the diffusion across epithelia. The behavior of the micelles will then depend upon their composition and general characteristics, such as size, superficial charge, shape, thermodynamic and kinetic stability. All these characteristics are essential to determine the fate of the micelles and the consequent drug bioavailability.

2.2.1. Size

The role of the size of nanocarriers in their biodistribution is very-well described in the literature [53,54] and has been more recently confirmed also in the case of polymeric micelles [55,56]. For instance, it has been proven that micelles with a size in the range from 30 to 100 nm can easily accumulate in highly permeable tumors, whereas poorly permeable tumors are pervaded only by micelles with dimension of 30 nm, hence-confirming the key role of size [57]. This could in principle be also true when considering the diffusion across the mucus layer or the uptake into epithelial cells, as reported for other nanosystems [58–60]. At our knowledge, however, no data are present in literature with respect to micelles. In this regard, it is also important to underline that, given their nature, micelles can disassembly in the mucus or in contact with epithelial cells and, in this case, the penetration ability will not depend upon micelles size but upon the characteristics of the unimers and by their specific interaction with mucus or cell membranes.

2.2.2. Surface characteristics

A relevant impact on micelles behavior is given also by surface characteristics, that regulate the stability upon i.v. injection as well as the interaction with mucus and epithelia. In agreement with the results obtained on solid polymeric nanoparticles [61], a hydrophilic and neutral surface reduces the formation of the protein corona [62] and increase the circulation time after intravenous injection. On the contrary, micelles with positive zeta potential are characterized by very low stability in biological fluids due to a non-specific protein binding and in an increased aggregation *in vivo* [63,64]. A neutral and hydrophilic surface also increases the mucus-penetrating properties [65–67], particularly relevant in the case of oral administration. On the other hand, positively charged nanocarriers are known for being mucoadhesive, better interacting with epithelia [68,69], and enhancing drug transport across biological barriers [39]. Finally, the micelle surface can be functionalized with specific molecules for active targeting, very useful in the case of chemotherapy [70,71].

2.2.3. Shape

Although micelles are commonly depicted as spherical systems, in some cases it is possible to observe the presence of rod-like, worm-like or even disk-like structures [22,72,73]. The differences in micellar shape are mainly related to the structure of polymers used [22,74] and to the characteristics of the surrounding environment in terms of temperature, pH and composition [74]. Micelles morphology study has been recognized as fundamental for predicting their behavior *in vivo* as the shape of these nanocarriers plays a key role in influencing circulation time, biodistribution and cellular uptake [73,75]. For instance, it has been proven that filomicelles, due to their elongated shape, flexibility and fragmentation capacity, are characterized by a slower clearance process and a prolonged circulation time than spherical micelles [76–78]. Recent data highlight that, at comparable diameter/cross-sections (40 nm), shorter filomicelles (length: 180 nm) showed the deepest tumor penetration and the most efficient cellular uptake in comparison with spherical micelles and long filomicelles (length: 2.5 μm) [79].

2.2.4. Micelle stability and drug release

Drug release from polymeric micelles can occur due to either drug diffusion from intact micelles or micelles disassembly (Fig. 4). In any case, to avoid an uncontrolled drug release at administration, micelles should have good thermodynamic as well as kinetic stability [33,80,81]. Therefore, several physicochemical strategies to avoid the rapid disaggregation of the system or to stabilize the encapsulated drug in the micellar core have been proposed, and are reviewed in a recent paper [82]. For instance, as it is well-known that a decrease in the CMC can be obtained by increasing the length of the hydrophobic portion of the unimer [22,33], block copolymers conjugated with a lipid molecule were synthetized. Other strategies comprise the functionalization of the hydrophobic block [83], the crosslinking of the micelle's core or the formation of a conjugate between the polymer and the drug in order to observe the drug release only after the bond breakdown. Micelles structural stability should be investigated also in biorelevant conditions, since plasma or intracellular fluids proteins can be absorbed on micelles surface leading to the formation of the so-called protein corona, which partially masks the outer shell functional groups modifying nanocarriers' physiological response in terms of biodistribution, cellular uptake, metabolism and toxicity [19,84–86]. In particular, serum proteins have demonstrated to play a key role on micelles stability by promoting their disruption or aggregation [63,87]. Other sources of instability for micelles have been found after their topical application to cutaneous and mucosal tissues [23,52]. Indeed, it is possible to observe micelles disaggregation as a result of the interaction with mucus, epithelia, stratum corneum lipids and sebum whereas the micelles interaction with the lacrimal fluid could cause drug precipitation as a result of the competition with solutes present in the tear film. Finally, it is worth underlying the intense ongoing research on stimuli-responsive polymeric micelles, capable of tuning drug release as a reaction to various impulses, both biological (such as acidic pH, redox potential or specific enzymes) and artificial, like ultrasounds, magnetic field, or temperature change [88].

2.2.5. Mechanisms of cell internalization

Considering the micelles' pivotal role in delivering drugs to a specific target at a subcellular level, several blindspots should be clarified regarding their internalization pathways [89,90]. The main pathway for micelles internalization is endocytosis, which is based on micelle interaction with cellular membrane, followed by the uptake in cells and the transport in endosomes in order to finally reach cells cytoplasm [89,91]. Really, in few cases polymeric micelles are internalized in their intact form: most of the times they undergo disassembling in the plasma membrane or are degraded in lysosomes [91]. In other words, micelles can enter cells as such, but they can also release the drug outside cells or be uptaken in form of disaggregated unimers, bringing to the accumulation of the drug in different sites like the plasma membrane or various cellular compartments [92,93]. The interest for micelles has been increased due to the fact that their internalization by endocytosis leads to an easy bypass of ATP-dependent efflux pumps reducing drug resistance as well as multidrug resistance (MDR) [94]. In addition to efflux

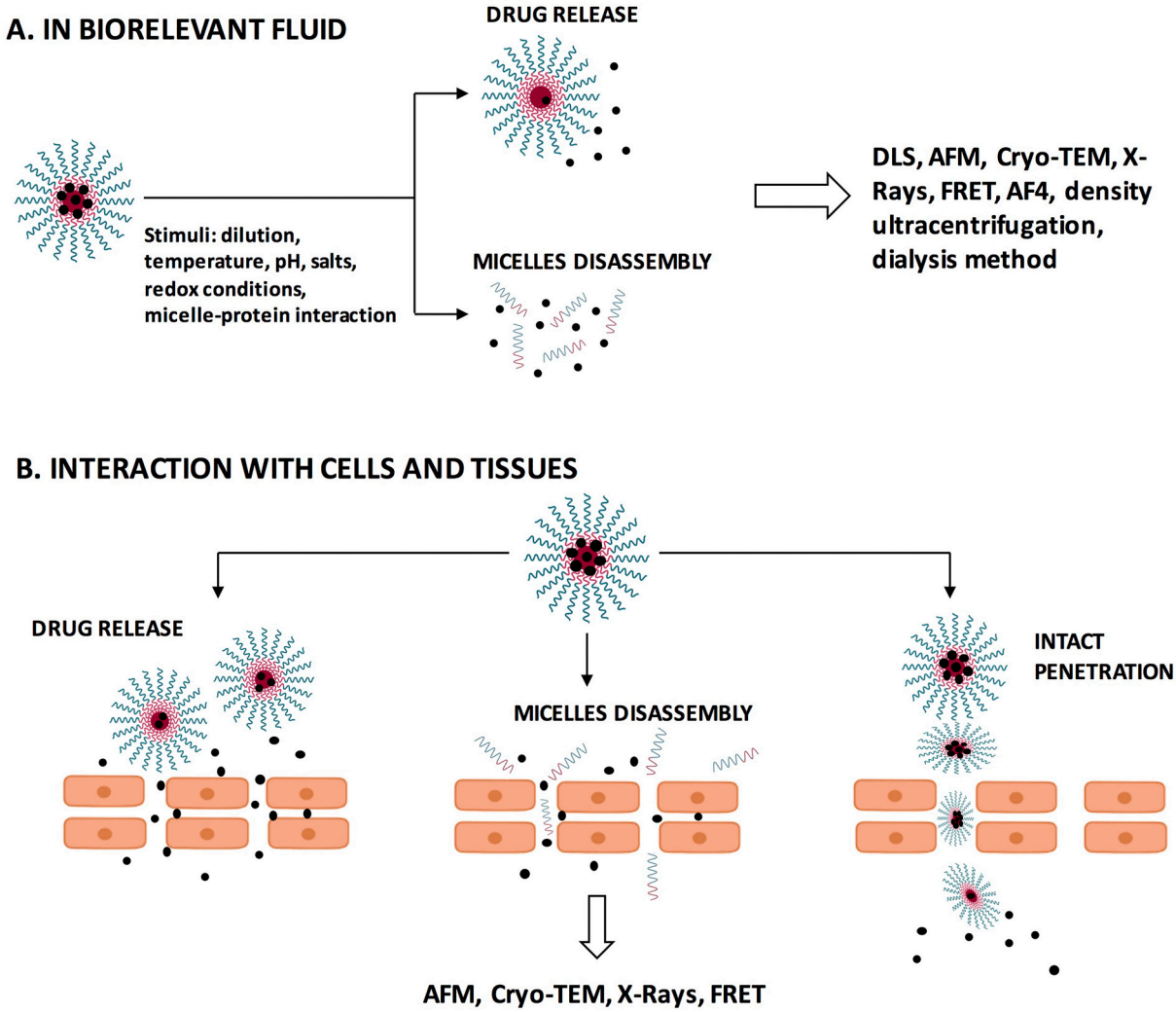

Fig. 4. Schematic representation of drug release and micelle interaction with the biological fluids (A) and with cells and tissues (B). In the figures, the techniques that could be used to study drug release are also indicated.

pumps diversion mediated by endocytic uptake, MDR can be strongly reduced by producing micelles made of polymers working as direct efflux pumps inhibitors (e.g. Pluronic®, D-α-Tocopheryl Polyethylene Glycol 1000 Succinate (TPGS), Soluplus®) [23,95–97] or by conjugating polymers with molecules (e.g. quercetin) having an inhibitory effect on these pumps [98]. In the first case, polymers inhibitory effect is not referred to micelles but directly to unimers which, increasing membrane fluidity, can cause an ATP depletion with consequent decrease of ATPase activity. Usually, the maximum inhibition of efflux pumps is registered at unimers concentration below the CMC [23].

3. Micelles characterization

Micelles characterization is of critical importance to define and predict their behavior in a biological environment. This task represents a real challenge, even more demanding compared to other nanocarriers, often requiring the combination of different approaches and techniques. The need for a thorough characterization, including the behavior in biorelevant media, has also been underlined in the EMA Reflection Paper on block copolymer micelle medicinal products [27].

In the following chapters, micelles characterization will be presented in detail. In particular, the first part will be dedicated to the investigation of CMC, drug loading and drug release from micelles by using several methodologies, whereas in the second paragraph the most important techniques used for micelles characterization will be briefly described, and their applications for the definition of micelles properties will be illustrated. For sake of clarity, Table 1 summarizes the different techniques that can be used to characterize micelles in terms of CMC, size, surface charge and morphology. In the same table, advantages and limitations of each technique are also briefly reported. Table 2 addresses the study of micelles kinetic stability, drug release and interaction with the biological environment, summarizing the different information that can be obtained.

3.1. Determination of CMC, drug loading and drug release

3.1.1. CMC

First, it is important to note that CMC value varies depending on the composition of the vehicle in which the polymer is dissolved and it cannot be assumed that the CMC in water or buffer is the same as the one in plasma or in another biological fluids. However, a single CMC value is often measured to characterize the system. CMC determination may be carried out through various methods, including the measurement of surface tension, the determination of probes absorbance [99] or fluorescence in solution [29], the measurement of the optical clarity or of the micelles' size by Dynamic Light Scattering [22,25,100].

The determination of CMC by measuring the solution surface tension is carried out through the Wilhelmy plate or the Du Noüy ring [100]. As

Table 1
Techniques used for the evaluation of micelles' CMC, size, surface charge and morphology, with a brief description of their advantages and limitations.

PROPERTY	TECHNIQUE	ADVANTAGES	LIMITATIONS	REF.
CMC	Surface tension	easy sample preparation	difficult data interpretation in case of some polymers (e.g. Pluronics) large sample volume time consuming measurement	[22,29,100–102]
	Absorbance (Sudan III, DPH) Fluorescence (Pyrene, Coumarin-6, Nile Red, DPH)	fast measurement high sensitivity	probes emission affected by environmental factors (e.g. solvent, temperature, pH and ionic strength)	[22,29,99,102–108,251]
	DLS	minimal sample preparation rapid and high through-put measurement	low sensitivity	[22,108,251]
Size and Morphology	DLS	non-destructive measurement minimal sample preparation avoidance of pre-experimental calibration high statistical accuracy time-dependent measurement rapid and high through-put measurement use of bio-relevant fluids	BIAS related to colored samples presence BIAS related to improper sample dilution possible interferences given by biorelevant fluids composition. resolution of multiple populations as a single contribution low accuracy and precision when measuring non-spherical micelles	[22,133,134]
	AFM	High resolution easy liquid sample preparation (avoidance of labeling, fixing or coating) possible evaluation of the different particle population	results slightly affected by sample preparation procedures or sample adsorption on support	[133,153,156–158]
	Cryo-TEM	high resolution (0.02 Å) avoidance of water removal with consequent reduction of artifacts low radiation damage investigation of morphological changes in media with different composition, pH or ionic strength	high sensitivity of sample preparation to conditions such as temperature and humidity expensive and time-consuming difficult set-up requiring highly skilled microscopists	[74,164–166,183,184]
	X-Rays	analysis of samples dispersed in a liquid sample amount in the range of tens of μl wide range of sample concentration short acquisition time evaluation of both spherical and non-spherical micelles	radiation damage limited access to X-rays facilities	[193]
Surface charge	DLS	See ADVANTAGES section of SIZE-DLS	See LIMITATIONS section of SIZE-DLS	[22,133,134]

described above, amphiphilic polymers in water-based solution behave exactly as surfactants reducing the interfacial free energy of the polymer-water system thanks to the minimization of the contact surface between the hydrophobic chains and the aqueous solution [22]. The decrease in system free energy goes hand in hand with the reduction of surface tension whose minimum value is reached at polymer concentrations corresponding to the CMC. Thus, measuring the surface tension of solutions at increasing amphiphiles concentrations, a decrease of the parameter can be observed until achieving a constant value once the CMC is reached. No significant surface tension change is observed at concentrations of polymer above the CMC [22,101]. For real, it has been proven that some polymers are characterized by a more complicated behavior which could lead to some difficulties in data interpretation. For instance, in the case of Pluronic® copolymers, the curve of surface tension against concentration showed two different breaks. The first one is related to the rearrangement of amphiphilic molecules at the air-water interface, while the second one represents the CMC value [100]. Other limitations of this technique are the long measurement time and the requirement of large sample volumes. Even though, the easy sample preparation makes the method highly appreciated for CMC determination [102].

In case of CMC measurement via absorbance or fluorescence techniques, a spectrometer or fluorimeter is used for detecting the signal produced by a dye added to solutions with increasing concentrations of the amphiphilic polymer. The intensity of this signal varies according to the characteristics of the surrounding environment leading to CMC value identification [22,99]. One of the most common agents used for this aim is Sudan III, a lipophilic compound with very low water solubility. Below the CMC an heterogenous mixture with very low absorbance is obtained as a result of dye poor water-solubility, whereas an increased signal can be observed at higher concentration of amphiphiles as a result of micellization with consequent dye incorporation in their core [99]. Besides Sudan III, other probes can be used including coumarin-6 [29], Nile Red [103], 1,6-diphenyl-1,3,5-hexatriene (DPH) [104,105] and pyrene, an hydrophobic fluorophore indicated as one of the most suitable dyes because of its ability to determine CMC values at very low polymer concentrations [22]. Even in this case, probe spectroscopic properties change according to the polarity of the surrounding environment reflecting its incorporation in the micellar core during micelles formation [22,106]. In particular, after pyrene loading in micelles, three changes can be observed: a red shift in the excitation spectrum from 332 nm to 338 nm, a decrease in the intensity ratio of the first and third vibrational peaks of pyrene (I1/I3) and an increase in the fluorescence lifetime from ~200 ns to ~350 ns [107]. Techniques based on dye signal detection are quite suitable for CMC determination because of their high sensitivity (CMC values lower than 0.1 mM) and fast measurement. Nevertheless, it should be always taken into account that the emission intensity is highly influenced by the probe photostability as well as the composition of the surrounding environment in terms of solvent used, temperature, pH and ionic strength [22,102].

Another technique is Static and Dynamic Light Scattering. In this case, samples with increasing polymer concentration are analyzed in order to plot the intensity values of scattered light against amphiphiles concentration. The scattered light depends linearly on the molecular mass of particles in solution. Below the CMC, the intensity shows a constant value corresponding to that of the dispersing medium, while a marked increase of scattered light can be detected at concentrations equal to the CMC, due to the formation of micelles in solution [35,108]. In order to follow micelles formation, it is also possible to monitor by Dynamic Light Scattering the correlation function signal. The intensity

Table 2
Summary of the different conditions in which micelles kinetic stability and drug/probe release can be evaluated, with regard of the information that can be collected and the techniques that can be used.

CONDITION	EXAMPLE	INFORMATION OBTAINED	TECHNIQUES
Buffer	PBS, HEPES, Acetate Buffer	Drug release over time Impact of pH and salt concentration.	Dialysis method [125,136] DLS [63,137,138], X-Rays [198,204,216], FRET [136]
Bio-relevant media	Buffer +albumins (BSA, FBS)	Protein corona formation; impact of on micelles stability and drug release	Dialysis method [127] DLS [139], X-Rays, FRET [233]
	Buffer + Glutathione Buffer + Enzymes	Triggered release (reducing agents/enzymes at the target site)	Dialysis method [63,131] DLS [145,148], X-Rays, FRET
	Buffer +bile salts Simulated gastric fluid Simulated intestinal fluid	Stability and drug release in the gastro-intestinal tract	Dialysis method [128,129] DLS, X-Rays, FRET
	Biological fluids (serum, cerebrospinal fluid, ascites fluid, pleural fluid, synovial fluid)	Evaluation of drug release and/or micelles disaggregation in complex matrices	AF4 [241], density ultracentrifugation [243], FRET
	Buffer+ mucins Mucus	Impact of mucin-micelles interaction on stability and drug release	DLS, X-Rays [212], FRET
Cells and tissues	Normal and cancer (es. MCF-7, M109, LNCaP) cell lines	Mechanisms of micelles-cell interaction: evaluation of intact penetration or micelle disassembly Accumulation in specific cellular compartments	FRET [92,162,220,234]
In-vivo studies	Post-sacrifice analysis of tissues Real-time analysis	Determination of micelles distribution/integrity in tissues Evaluation of micelles disassembly in the bloodstream	FRET [228] FRET [230,235–237]

of the correlation function gives information on the diffusion coefficient of particles in solution and then on their hydrodynamic size. At concentration below the CMC, the diffusion coefficient of monomers can't be measured, because of their too small size and low-intensity contribution. When CMC is reached, the intensity of the scattered light strongly increases and the correlation function allows to determine the hydrodynamic size of aggregated micelles. [108]. Even if DLS has been indicated as a rapid, high-throughput tool for CMC determination, the technique presents some limits including the possibility to analyze only samples with relatively high polymer concentrations (above 50 ppm) [22]. Further details on this technique are presented in chapter 3.2.1.

3.1.2. Drug loading

Polymeric micelles are characterized by an anisotropic distribution of water, whose content decreases moving from the surface to the core, which is hydrophobic. Thus, drug localization inside the micelles depends on their polarity: hydrophobic APIs will be solubilized in the micellar lipophilic core while molecules with intermediate polarity or highly hydrophilic will be located respectively in an intermediate position or on the surface of the system [109,110]. Actually, hydrophilic molecules are mostly loaded by chemical conjugation with the unimers, or via electrostatic interactions by using polyion complex micelles. For instance, RNA is generally loaded through the incorporation of polycations in the structure of amphiphilic block copolymers and then used for RNA condensation [111,112]. Concerning hydrophobic drugs, the amount loaded strictly depends on the hydrophobic interactions occurring between the drug and the micellar core. The length of the polymers hydrophobic chain, in addition to the type and level of substituents, is pivotal for defining the degree of encapsulation [22,81].

The definition of the loading capacity, also called drug loading (DL), and the entrapment efficiency (EE) should be carried out to evaluate the suitability of the excipients as well as to select the preparation method ensuring an efficient encapsulation of the selected drug. DL and EE can be calculated as:

$$\%\mathrm{DL} = \frac{amount\ of\ drug\ in\ the\ micelles}{total\ micelles\ weight\ (drug + polymer)} \times 100$$

$$\%\mathrm{EE} = \frac{amount\ of\ drug\ in\ the\ micelles}{total\ amount\ of\ drug\ initially\ added} \times 100$$

where the amount of drug in the micelles, in case of lipophilic compounds, can be quantified spectrophotometrically or via HPLC analysis after separation of the undissolved drug. Indeed, for hydrophobic drugs the water solubility of the loaded compound is generally so low that it is not necessary to differentiate between the drug present free in solution and the encapsulated amount. In the case of hydrophilic molecules, the separation between free and encapsulated compound can be obtained by using ultrafiltration spin columns with an appropriate cut-off (lower than micelle's size and higher than drug size) [113]. Some authors evaluated the encapsulation efficiency of volatile hydrophilic compounds by Gas Chromatography, since, as a result of drug–polymeric micelle interactions, a decrease of the amount of free volatile compounds in bulk water was found [114].

3.1.3. Drug release studies

Drug release studies from polymeric micelles are performed to evaluate the impact of excipients and manufacturing methods on drug release during formulation development, and as quality control to support batch release. Additionally, when micelles are designed to provide a targeted delivery in specific environmental conditions, these studies are fundamental for confirming the effective release of the drug in the presence of the triggering stimulus [115].

Drug release from nanocarriers cannot be studied with conventional methods, due to the impossibility to separate by filtration the encapsulated drug from the released one. For this reason, non-compendial approaches are used, where the separation of the released drug from the encapsulated one is generally done either by using a dialysis membrane or by ultracentrifugation or ultrafiltration. Even if these methods are indicated in the literature as suitable for drug release evaluation, each and every one has limitations, and the method selection is made on a case by case basis [116]. The interest for this issue, as well as the challenges involved, have brought to the publication of different reviews where the release methods for nanocarriers are discussed [117,118] and novel strategies (*e.g.* voltammetry and turbidimetry) are also described. We refer the readers to these papers for a thoughtful discussion on this topic.

The most common method used for describing drug release from micelles is the dialysis one. Briefly, the micellar formulation is introduced into a dialysis bag which is immersed in a recipient filled with the release medium maintained at constant temperature and stirring speed. While the released drug can diffuse from inside the bag to the outer medium, the micelle is prevented to cross the membrane due to its size. Therefore, by analyzing samples withdrawn from the external medium at different time points, the release profile can be built [80,117,119]. To ensure the correctness of the results, the volume and the composition of the acceptor medium should be selected to guarantee sink conditions;

most of the times the formulation volume inside the membrane is in the range 1-10 ml, while the outer volume is between 40 and 90 ml [117,119]. Moreover, an adequate cut-off must be chosen to assure the complete release of the drug; while small molecules easily diffuse across dialysis membranes, large cut-off values are necessary in the case of proteins and antibodies [119]. Possible drug-membrane interaction should also be evaluated. Finally, it should be always considered that the amount of drug found in the receptor compartment is the result of two processes: the effective release of the drug from the micelle and the permeation of the drug across the dialysis membrane [120]. Thus, results of drug release from nanocarriers should always be compared with those coming from a reference solution of the drug alone [121], to determine the diffusion barrier properties of the dialysis membrane. This approach, combined with adequate mathematical models, can be used to predict the actual release kinetic from micelles [117,122].

In specific cases, release studies could be carried out without dialysis membrane; it is the case of polarity-sensitive fluorescent probes and FRET (Foerster resonance energy transfer) use (see specific chapter) [63,91,123,124].

3.1.3.1. Drug release studies in biorelevant conditions. Most of the times, a drug release study is performed to collect general information about micelles behavior in very common buffers such as PBS (Phosphate Buffered Saline buffer) and HEPES (4-(2-hydroxyethyl)-1-piperazineethanesulfonic acid buffer), with the main aim to select the more appropriate polymers for micelles' development or to investigate the mechanisms of drug release. For example, a study was conducted by San Miguel *et al.* [125] to analyze the effects of the length of the hydrophilic block of three block copolymers on drug incorporation and release. The drug was the anticancer chlorambucil (characterized by low water solubility) loaded in polymeric micelles composed of 2-(N,N-dimethylamino)ethyl methacrylate (PDMAEMA, hydrophilic block, constituting the external shell) and ε-caprolactone (CI, hydrophobic block, constituting the micellar core). The release profiles, that differed depending on the length of PDMAEMA blocks (polymerization degree: 20, 25 or 30) (Fig. 5A), helped to figure out the mechanisms involved in the release, *i.e.* a combination of degradation and diffusion (See Fig. 4).

Although an overview about drug release can be obtained by using standard buffers, the *in vitro* behavior of micelles is quite different from the one registered after administration due to the more complicated composition of biological fluids. On these bases, investigation of drug release from micelles in bio-relevant media with different components should be performed to collect a clearer picture of their *in vivo* behavior. For instance, Liu *et al.* [127] studied the release of an anticancer drug, ellipticine, from micelles composed of (polyethylene glycol)-b-poly (5-benzyloxy-trimethylene carbonate; MePEG-b-PBTMC 5000-b-4800) (MePEG-b-PBTMC) in the absence and presence of bovine serum albumin (BSA) at 37°C to assess the influence of serum protein on the drug release profile. The dialysis bag (MWCO= 100000 Da) was filled with a mixture of drug and BSA in PBS at pH 7.4 whereas a 45g/l of BSA solution in PBS was used as the receptor. At different time-points, 20 μl of solution were withdrawn from inside the dialysis bag and ellipticine concentration was quantified via fluorescence method. The external medium loaded with 45 mg/l BSA remarkably increases the release of the drug in comparison to the same medium without the protein, thus confirming the strong impact of protein-drug interactions on the release profile.

Other Authors determined drug release profile in buffers reproducing gastro-intestinal tract conditions to examine micelles attitude to disaggregate or release the cargo when orally administered. Particularly, media such as the Fasted State Simulated Gastric Fluid (FASSGF) simulating physiological conditions in the stomach at the fasted state, the Fasted State Simulated Intestinal Fluid (FASSIF) reproducing upper intestine conditions or buffers enriched in bile acids could be employed [128,129]. For example, Van Hasselt *et al.* [129] described vitamin K release profile from polymeric micelles by using dialysis bags containing buffers with different concentrations of bile salts to define a possible improvement of vitamin K intestinal absorption using micelles.

Drug release studies can also be used as a proof-of-concept of the stimuli-responsiveness of the micellar systems. Stimuli that change micelles structure and trigger drug release are for instance pH (typically lower in endosomes/lysosomes, in tumor cells and in inflamed tissues), presence of reducing agents (such as glutathione, whose level is quite elevated in some tumors), specific enzymes (for instance matrix metalloproteinases overexpressed at tumor sites or matrix metalloproteinases-13, overexpressed in osteoarthritis) or also external stimuli such as ultrasounds, temperature and light [115,130]. Particularly, Zhu and co-authors [63] measured the release profile of doxorubicin-loaded polymeric micelles. As shown in Fig. 5B, at pH 7.4 less than 25% of doxorubicin was released, whereas at pH 5.5, reproducing the endosomal and lysosomal conditions, an improved release was observed. Finally, in presence of 10 mM glutathione (GSH), reproducing tumor cells environment, characterized by abnormal redox conditions, more than 70% and more than 90% of the drug was released respectively after 12 h and 36 h of incubation (Fig. 5B).

Other authors developed pH-sensitive and enzyme-sensitive doxorubicin-loaded micelles [126,131]. Gao *et al.* [131] prepared micelles made of modified alginate for cancerous tissues targeting, and evaluated drug release in different pH conditions and in presence of alpha-L-fucosidase (AFU), a lysosomal enzyme overexpressed in some tumors like hepatocellular carcinoma. As the enzyme works as a trigger for

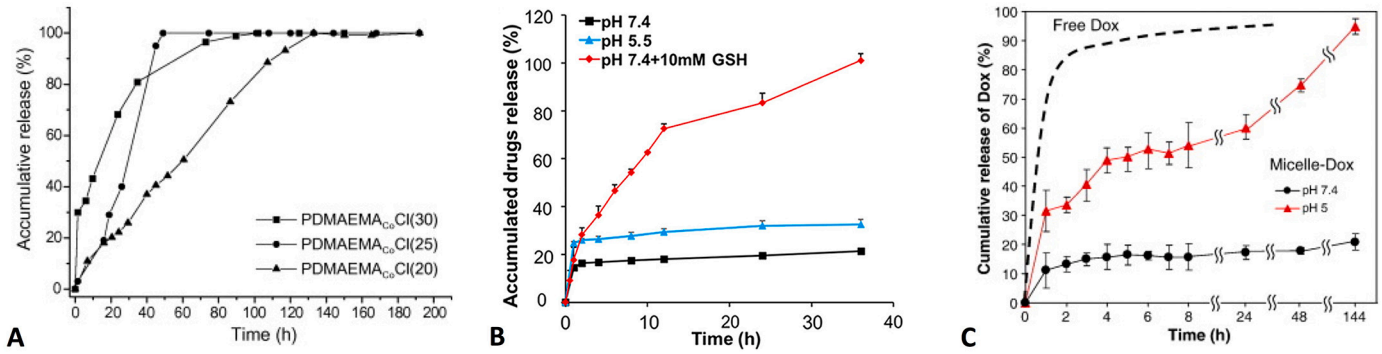

Fig. 5. Release profile of drugs from polymeric micelles. The release experiment is performed for selecting the best polymeric composition or for demonstrating a triggered release. Panel (A): chlorambucil release from micelles composed of PDMAEMACoCl(30), PDMAEMACoCl(25) or PDMAEMACoCl(20) in 0.01 M PBS pH 7.4. Reprinted from [125] with permission of Elsevier. Panel (B): doxorubicin release from micelles in PBS at different pH (7.4 and 5.5) and in PBS (pH 7.4) added with 10 mM glutathione, working as reducing agent. Adapted with permission from [63]. Copyright (2018) American Chemical Society. Panel (C): doxorubicin release from PEG-b-PEYM micelles at pH 7.4 and 5. Drug release is triggered by acidic pH, due to the presence of acid-labile ortho ester side-chains in the polymer. Reprinted from [126] with permission of Elsevier.

micelles disassembly, a dramatic enhancement in doxorubicin release was found at pH 5.5 in presence of AFU. Similar results were obtained using PEG-b-PEYM (poly(ethylene glycol)-block-polymethacrylate) micelles: drug release is triggered by acidic pH, due to the presence of acid-labile ortho ester side-chains in the polymer (Fig. 5C) [126]. Finally, drug release from light-sensitive micelles can be evaluated via common methods such as the dialysis one by maintaining the samples under irradiation during the experiment [132].

3.2. Techniques used for micelles characterization

3.2.1. Dynamic Light Scattering (DLS)

Dynamic Light Scattering (also known as Photon Correlation Spectroscopy) is a fundamental technique for the determination of the size and surface charge of nanocarriers. In the case of size, the determination by DLS is carried out exploiting colloidal dispersions Brownian motions, defined as random motions related to the size of particles and to the viscosity and temperature of the medium. Thus, hitting the sample with a monochromatic beam of light, the scattered light at a given angle displays fluctuations in time, with a characteristic time related to the diffusion coefficient of the micelles in solution. The hydrodynamic radius RH of the micelles can be calculated from the measure of the diffusion coefficient D via the Stokes-Einstein equation $D \div R_H^{-1}$. Regarding surface charge, or, more properly, zeta potential determination, the principle is basically the measure of the hydrodynamic diameter of micelles in solution under the effect of an electric field, affecting the diffusion of particles as a function of their surface charge. DLS advantages are the non-invasive measurement, the minimal sample preparation, and the avoidance of pre-experimental calibration [133]. In addition, modern instrumentations can produce time-dependent measurements and detailed quality reports of the collected data in order to define their correctness [133,134]. Although the easy-to-handle technique, some limitations should be considered. Firstly, the need to avoid the analysis of colored or fluorescent samples which could partially absorb the energy of the monochromatic light leading to an underestimation of the particles size. Secondly, to ensure good results of the analysis, proper dilution is fundamental to prevent dilution under the CMC value and to minimize multi-scattering phenomenon taking place at high sample concentration. In addition to the limitations described above, another weakness of DLS is its narrow resolution, preventing the possibility to recognize particles differing from each other for a factor lower than 3 (*e.g.* particles of 90 and 110 nm are not distinguished and a very high polydispersity index (PDI) is obtained) negatively impacting on the correctness of data obtained from polydisperse samples measurement [133]. In this regard, it is possible to couple DLS with a separation technique (such as Asymmetrical flow field-flow fractionation, see par. 3.2.6) to overcome this problem. Finally, as DLS instrumentation has been developed and optimized for spherical nanosystems, when measuring non-spherical particles, the obtained results can be characterized by low accuracy and precision [134].

3.2.1.1. DLS for micelles size and surface charge determination in biorelevant conditions. As size and surface charge are involved in the regulation of the biodistribution and pharmacokinetic properties of micellar systems, their determination by DLS is fundamental to predict micelles behavior when in contact with body fluids and tissues [22,64]. Preliminary DLS measurements during formulation development are generally performed in water or in a buffer, where the simple vehicle permits to assess the effect of drug incorporation on micelles size and charge. However, to be able to better predict *in vivo* micelles behavior, DLS analysis in more complex media can be performed. Additionally, in the case of stimuli-responsive micelles, this technique can give preliminary information regarding nanocarriers behavior when undergoing pH or other environmental conditions variations [135,136].

DLS can be used as well for evaluating micelles tendency to aggregate or disassembly over time as done by Moretton and collaborators [137] who determined the size of both blank and rifampicin-loaded micelles composed of poly(epsilon-caprolactone)-*b*-poly (ethylene glycol)-poly(epsilon-caprolactone) (PCL-PEG-PCL) in filtered water at predetermined time intervals for one week after incubation of samples at 25°C. A similar evaluation of micelles stability over time was performed by Garg *et al.* [138]. Briefly, micelles were incubated in PBS solution (pH 7.4) containing 0.01% (w/v) sodium azide at 37°C and their hydrodynamic diameter and PDI were measured over a period of 100 days. The stability of these micellar systems was studied also in presence of SDS, used as a destabilizing agent. Comparing the size peak intensity and the hydrodynamic diameter obtained in the stability experiment with the values obtained in presence of SDS, it was possible to identify micelles eventual disaggregation.

Regarding zeta potential, Zhu *et al.* [63] investigated the surface charge of doxorubicine-loaded polymeric micelles when in contact with PBS at different pH (7.4, 6.2, 5.5, 5.0 and 4.5) in order to explore the endosomal escape capacity of the system, which should increase with protonation. Zeta potential values were found to be -34.52 ± 0.15, -30.23 ± 0.38, -24.94 ± 1.13, -12.80 ± 0.33, and -2.72 ± 0.15 mV respectively, confirming the possibility to improve the endosomal escape process using these micelles.

With regard to more biorelevant media, Ebrahim Attia *et al.* [139], measured the size of doxorubicin-loaded poly(ethylene glycol) (PEG) micelles in 10% fetal bovine serum (FBS) solution over 48 hours to exclude possible precipitation or aggregation at physiological conditions, confirming micelles stability. Furthermore, Sun *et al.* [140] measured 9-nitro-20(S)-camptothecin-loaded polymeric micelles at different time points (0.5, 2, 6, 12, and 24 h) in PBS pH 7.4, in acetate buffer pH 5 (mimicking tumor cells microenvironment) and in the presence of cathepsin B in pH 5.0 (mimicking tumoral lysosomes). In PBS and acetate buffer, micelles were monodispersed and stable over time. On the contrary, after incubation with cathepsin B at pH 5.0, the same samples yielded two different size peaks and a decrease in diameter probably originated by secondary micelles formation caused by cathepsin.

Concerning stimuli-responsive micelles, DLS showed its usefulness in defining micelles structural modifications in response to temperature [141–143], pH [143,144], enzymes [145,146] and light [141,147]. Li and its research group [148] have nicely demonstrated the capability of redox-sensitive hyaluronic acid-deoxycholic acid (HA-ss-DOCA) micelles to modify structure and size as a function of glutathione concentration. Similarly, this technique has been used to demonstrate the disassembly of micelles having a poly(propylene sulfide) (PPS) hydrophobic core, following H_2O_2 treatment. Oxidation of the PPS core made it more hydrophilic and triggered micelle disassembly. This evidence, combined with TEM and FRET data, supports the use of these stimuli-responsive micelles for site-specific drug delivery to tissues characterized by high levels of oxidative stress [136]. Another example is represented by the size of metalloproteinases-sensitive micelles composed of biotin-poly(ethylene glycol)-blocked-poly(L-lysine) (PEG-*b*-PLL) and conjugated with doxorubicin [145]. DLS analysis confirmed the morphological changes resulting from micelles breakage induced by the enzymatic cleavage of the peptide linkage between doxorubicin and PLL.

Although DLS has demonstrated interesting applications in the field of micelles size, surface charge and stability determination in physiological conditions, the use of media enriched with vitamins, lipids, protein or other macromolecules could interfere with DLS measurement making data interpretation difficult [133]. For this reason, DLS can be used coupled with separation techniques as in the case of asymmetric flow field-flow fractionation (AF4) (see par. 3.2.6).

3.2.2. Atomic Force Microscopy (AFM)

Atomic Force Microscopy (also known as Scanning Force Microscopy) is a very high-resolution type of Scanning Probe Microscopy

(SPM) used for the determination of morphology and size of nano-systems, including micelles. The technique is based on the deposition of the sample as thin layer on a support which is scanned by a very sharp tip probe mounted on a cantilever deflecting differently according to the topography of the sample. As the cantilever is hit by a laser beam for the entire time of the measurement, sample morphology reconstruction occurs thanks to the scattering of this laser beam due to cantilever deflection [149,150]. In order to ensure good results of the measurement, the specimen should be strongly attached to the solid support surface to resist the lateral forces exerted by the scanning tip which could move, sweep or drag the specimen producing important artifacts concerning nano-systems morphology [151]. This is particularly relevant in the case of micelles, which could be disrupted by fragmentation into monomers. For this reason, the tapping mode, a procedure that is known to minimize the sample distortion due to mechanical interactions between the AFM tip and the surface, is sometimes used. Substrates such as mica, glass and silicon oxide have the best performances for the easy adsorption of the sample on their surface as well as the possible covering with thin lipid films mimicking biological substrates for the investigation of aspects including molecular recognition, cell adhesion and membrane fusion. Regarding samples immobilization on the support, the most common procedures are based on the deposition of a drop of an aqueous solution containing the nano-system followed by water evaporation or drying with liquid nitrogen. In other cases, strategies such as the immersion of substrates in the solution of interest or the spraying of an aqueous solution onto the support can be used [152]. AFM appeal in the field of nanocarriers characterization is related to the possibility to analyze highly complex samples avoiding actions such as labeling, fixing or coating, in addition to the very high resolution, approximately of 0.1 nm [153]. Even if imaging can be obtained also in aqueous solution, most of the times images have been collected after solvent evaporation.

3.2.2.1. AFM as tool for micelles size and morphology determination. AFM has been indicated as a proper tool for micelles size determination due to its ability to distinguish particles with different dimensions in a mixture as well as to operate at room temperature, thus allowing the analysis of biological samples close to native and physiological conditions [133,154–156]. Generally, the size obtained by using AFM results slightly lower compared to DLS analysis, probably because AFM technique measures the diameter of particles when collapsed after solvent evaporation whereas DLS focuses on the determination of the hydrodynamic diameter, that is sensitive to corona swelling caused by the solvent. Indeed, the size of curcumin-loaded monomethoxypoly (ethylene glycol)-poly(ε-caprolactone) (mPEG-PCL) micelles [157] was found to be 89.0 nm by AFM and 98.0 nm by DLS, respectively. Similarly, the size of micelles made by linear poly(styrene-*b*-isoprene) (PS−PI) described in the work of Minatti *et al.* [158] resulted 40 ± 0.6 nm by AFM , while *approx.* 50 nm by DLS. Concurrently with size determination, Minatti and co-workers used AFM to investigate the effect of the cyclization of PS−PI copolymer on the morphology of micelles. AFM samples were prepared by solvent casting starting from micellar solutions of linear or cyclic PS-PI at different concentration. In case of linear PS-PI, the concentration did not influence micelles shape but strongly impact on micelles packing. Indeed, at low concentrations (0.1 mg/ml, Fig. 6A) micelles were found as individually dispersed or organized in small clusters, at 1 mg/ml (Fig. 6B) it was possible to observe a quite dense packing and at 5 mg/ml a uniform layer was reached (Fig. 6C). A different behavior was observed in case of cyclic copolymer. At concentration of 0.1 mg/ml, micelles had the same shape as before (Fig. 6D) whereas at concentration of 1 mg/ml they were both cylindric and wormlike instead of spherical (Fig. 6E). Finally, at concentration of 5 mg/ml it was possible to observe only wormlike micelles (Fig. 6F).

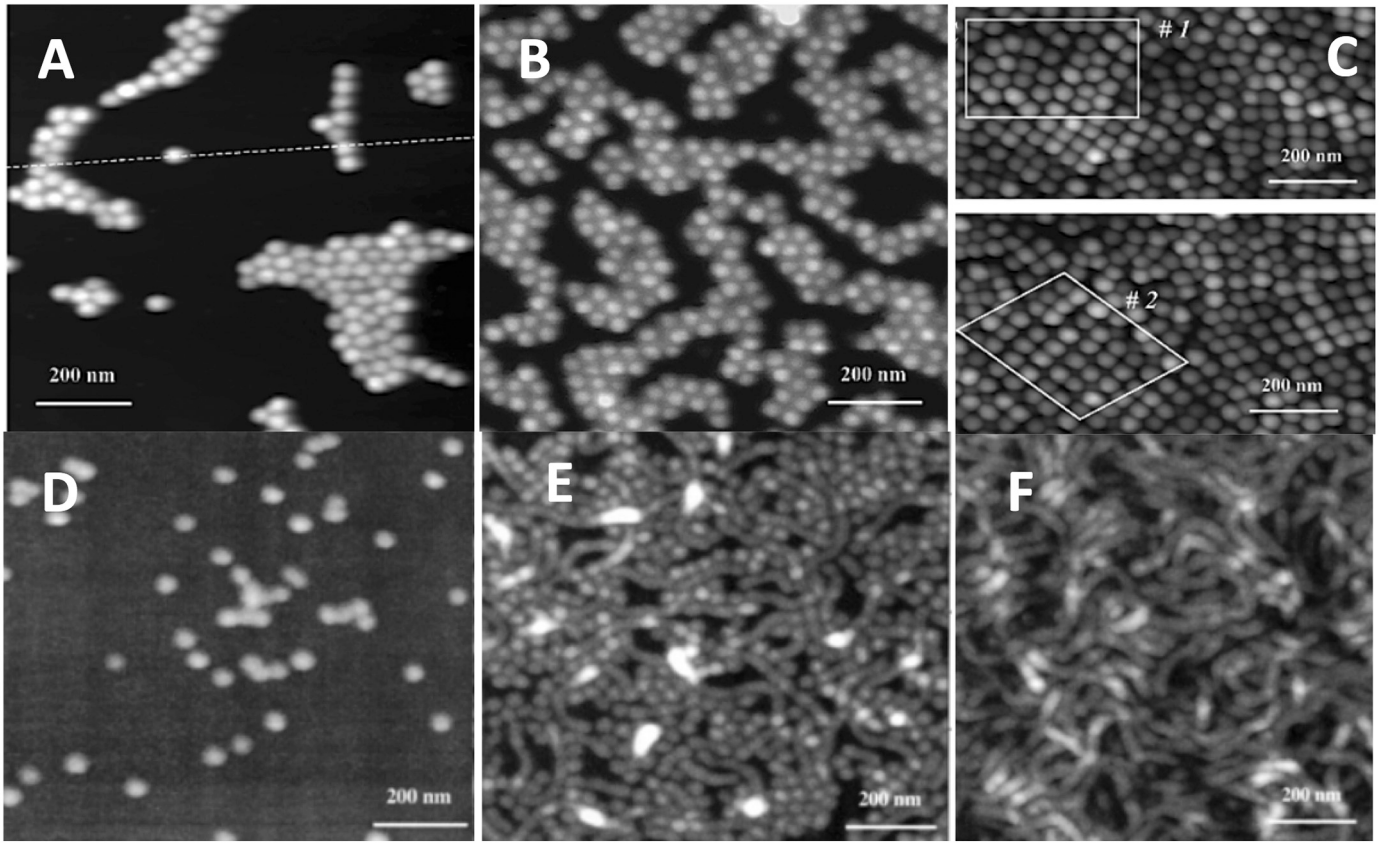

Fig. 6. AFM images (1 × 1 μm^2) of linear (A, B, C) and cyclic (D, E, F) poly(styrene-b-isoprene) (PS−PI) micelles obtained from solutions in heptane. Polymer concentration was 0.1 mg/ml (A, D) 1 mg/ml, (B, E) and 5 mg/ml (C, F). Adapted with permission from [158]. Copyright (2003) American Chemical Society.

Similarly, AFM has been used to evaluate the impact of drug loading on the morphology of micelles composed of poly(2-n-butyl-2-oxazoline). While at 10/0.2 polymer/drug (paclitaxel) ratio worm-like micelles were present, at 10/5, micelles turned to spherical with an average diameter of 40-50 nm [159], allowing to describe the correlation between drug loading and micelles morphological features.

3.2.2.2. AFM for evaluating micelles stimuli-induced morphological changes and interaction with biological systems. AFM could also be a promising strategy for exploring micelles temperature-related or redox-related morphological changes. For example, Kohori *et al.* [160] evaluated the structural modifications of thermo-responsive block copolymer micelles after drying at 4°C and 40°C, pointing out the presence of rounded-shape individually dispersed micelles at 4°C in contrast with aggregated systems, often retaining their spherical shape, at the higher temperature. Furthermore, Li and its research group [148] investigated disaggregative behavior of redox-sensitive polymeric micelles for delivering the anti-tumor drug paclitaxel. Micelles morphological changes were studied after 24 h incubation with 10 μM, 10 mM and 20 mM glutathione (GSH) to reproduce respectively human plasma GSH concentration (10 μM) and tumor environment (10 and 20 mM). For micelles treated with 10 μM GSH no significant morphological change was observed in comparison to untreated micelles. On the contrary, micelles incubated with 10 mM and 20 mM GSH were characterized by irregular shape and bigger size as a result of an increased aggregation caused by micelles disruption in reducing conditions.

AFM has also been proposed as innovative tool for studying the mechanisms regulating nanocarrier interaction with cell membrane and their internalization, which are quite relevant for ensuring effective drug delivery to the target [161–163]. For instance, Vasir *et al.* [161] analyzed the role of surface functionalization with poly-L-lysine on the cellular uptake of poly-(d,l-lactide-*co*-glycolide) (PLGA) nanoparticles (NPs). Cells were incubated with both functionalized and not functionalized NPs and they were visualized by liquid imaging in tapping mode as samples fixation to the AFM support can prevent the observation of cells morphological changes. Results showed complete disappearance of functionalized NPs from cellular surface after 20 minutes-treatment whereas not-modified NPs were still covering the cell surface, demonstrating a faster internalization for functionalized NPs. This paper refers to polymeric nanoparticle, but this technique (i.e. AFM analysis of cell surface to follow nanocarriers fate) could be also applied to polymeric micelles. Indeed, Xiao *et al.* [162] studied cells behavior after 1 h treatment with blank and Nile-red-loaded poly(ethylene glycol)-poly (lactic acid) (PEG-*b*-PLA) micelles. AFM images of treated cells showed a much rougher surface than the one of untreated cells, demonstrating micelles possible interactions with cellular membranes during the internalization process.

3.2.3. Cryo-Transmission Electron Microscopy (Cryo-TEM) and Transmission Electron Microscopy (TEM)

Due to the high resolution (0.02 Å) and easy sample preparation [74,164], Cryo-Transmission Electron Microscopy has recently emerged as a powerful tool for describing the morphology of micelles. The structural characterization of samples, following the same principles of Transmission Electron Microscopy (TEM), is obtained by striking the specimen with a beam of electrons which interacts with nano-scale components leading to a detailed visualization of samples main characteristics [164]. However, while TEM imaging requires complete samples dehydration in order to ensure high vacuum in the microscope column, cryo-TEM is based on the rapid freezing of samples at temperatures of at least -170°C using liquid nitrogen, liquid propane or liquid helium [74,164], allowing for the observation of specimens in their hydrated and native state and reducing artifacts related to water removal [74,165,166]. As micelles are dynamic structures whose morphology strictly depends on the characteristics of the surrounding environment [72,167], avoidance of water elimination is one of the main reasons why cryo-TEM is preferred to other imaging techniques. Moreover, as the analysis of samples at cryogenic temperatures remarkably reduces the extent of radiation damage, imaging resolution can be easily improved by increasing the electron dose used [164]. Finally, cryo-TEM is an interesting tool for colloids internal structure investigation *via* the freeze-fracture technique, consisting of breaking apart the frozen sample in order to expose its core to the electronic microscope analysis [168]. Although several advantages of this approach, maintenance of controlled conditions is strictly required for collecting reproducible data; thus, it should be always taken into account that during specimen preparation a rigorous control of environmental conditions including temperature and humidity rate is necessary [74,166]. Moreover, cryo-TEM is a very expensive and time-consuming technique with a difficult set-up requiring highly skilled microscopists [169]. For this reason, despite cryo-TEM is recognized as a more suitable tool for micelles imaging than standard TEM, the majority of micelles morphological evaluations found in the literature are performed by using TEM, whose results often (even if not always [170]) demonstrated to be in agreement with cryo-TEM observations [169,171]. For instance, Petzetakis *et al.* [171] used both TEM and cryo-TEM for analyzing the morphology of micelles made of poly(lactide)-b-poly(acrylic acid) copolymer (PLA-*b*-PAA) containing its PLA block in form of pure enantiomers as well as racemic mixture. By using standard TEM, micelles appeared cylindrical for enantiomers, whereas in case of the racemic mixture spherical nanostructures were visualized. The same morphological differences between the two populations of micelles were found also by observation with cryo-TEM, providing confidence for TEM use. In addition to this, standard TEM can have interesting application for the determination of the cellular fate of micelles labeled with heavy atoms such as gold [90,172] or radioactive probes [90].

3.2.3.1. Cryo-TEM for morphology studies and for the evaluation of stimuli-induced morphological changes. Cryo-TEM can be used as an effective imaging tool for understanding the influence of polymers and/or cargo on micelles shape [173,174]. For instance, the technique was used by Janas *et al.* [175] to describe the morphology of dexamethasone-loaded micelles prepared by using novel block co-polymers made by an hydrophilic block of methoxy-polyethylene glycol (mPEG) and a lipophilic block composed by either n-butyl methacrylate monomer (BuMA), or benzyl methacrylate monomer (BzMA) and/or 4-acrylamido benzoic acid monomer (AAmBzA). Thanks to the cryo-TEM images (Fig. 7) it was possible to appreciate the influence of the composition of the hydrophobic block on micelles morphology, and to observe dexamethasone in the micellar core, confirming drug loading in the nanocarrier.

Furthermore, Cryo-TEM has demonstrated to be quite interesting for determining the impact of polymer concentration on micelles shape. Particularly, Fairley *et al.* [176] studied by TEM the assembling behavior of the amphiphilic copolymer PEG_{5000}-*b*-PCL_{4100} at concentration of 50 mg/ml, 25 mg/ml, 2 mg/ml and 0.5 mg/ml and used Cryo-TEM to confirm that the morphologies found by TEM actually existed in solution. TEM images showed micelles with spherical shape at a concentration of 50 mg/ml, sphere-to-rod transition after dilution to 25 mg/ml, different micellar morphologies, including lamellar sheets, shorter rods and smaller spheres at concentration of 2 mg/ml, while at 0.5 mg/ml only longer rods and spheres were visualized (Fig. 8).

As micelles morphology depends on the characteristics of the surrounding environment, and cryo-TEM is able to preserve the hydrated micellar shape, it is an ideal technique for the study of stimuli-induced morphological changes. At the moment, however, very few studies can be found on this topic, and, for this reason, the examples here reported mainly concern either micelles made of low MW surfactants, or polymeric micelles used for applications other than drug delivery and, often, in non-physiological conditions. Nonetheless, the potential of this

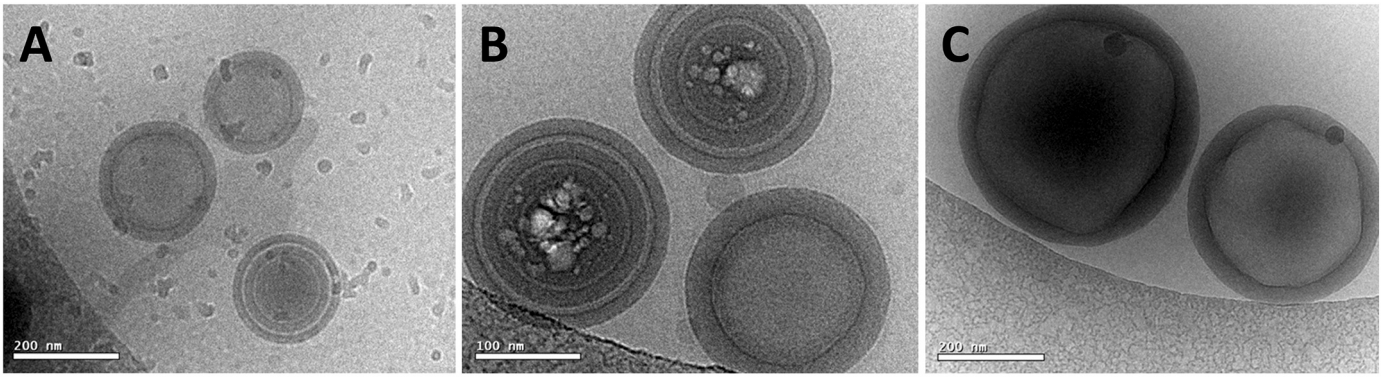

Fig. 7. Blank micelles (A) and dexamethasone-loaded micelles (B) of block copolymer composed of α-Methoxy-polyethylene glycol (mPEG), n-butyl methacrylate monomer (BuMA) and benzyl methacrylate monomer (BzMA). Panel (C) illustrates dexamethasone-loaded micelles of a block copolymer composed of mPEG, (BuMA) and 4-acrylamido benzoic acid monomer (AAmBzA). Adapted from [175] with permission of Elsevier.

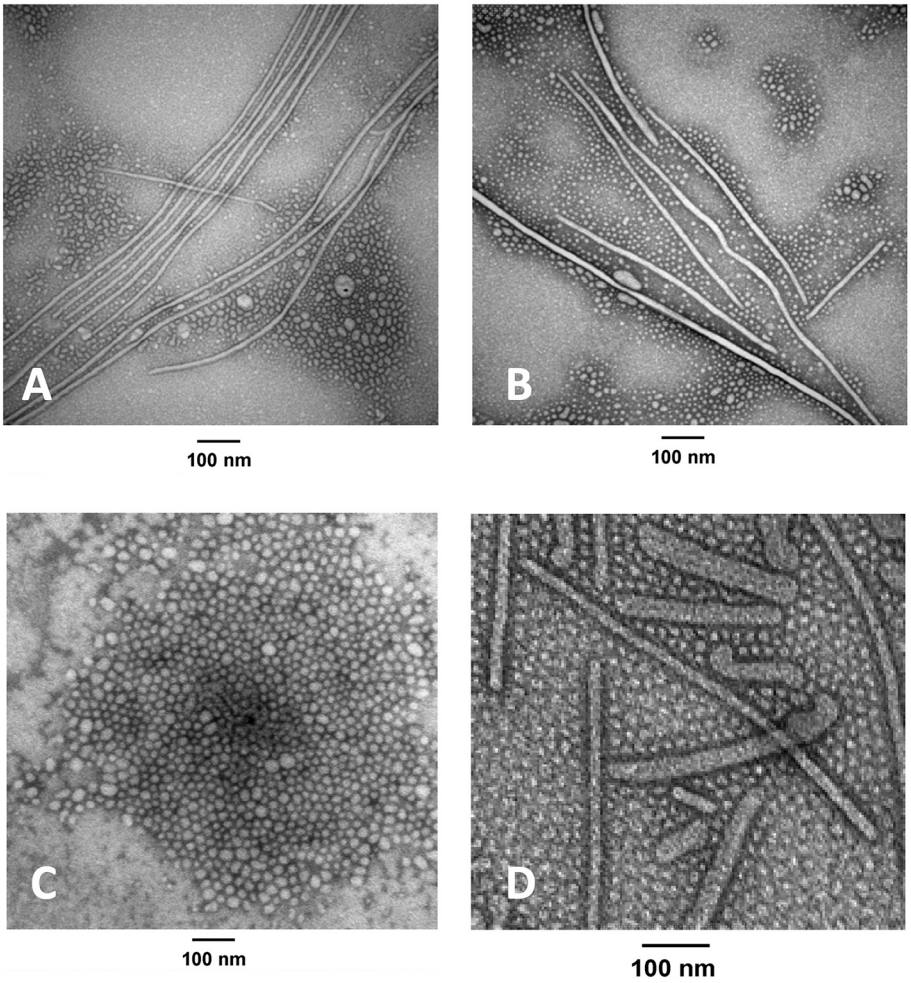

Fig. 8. TEM images of micelles at different polymer (PEG_{5000}-*b*-PCL_{4100}) concentration: 0.5 mg/ml (A), 2 mg/ml (B) and 50 mg/ml (C). Panel (D) illustrates a Cryo-TEM image related to 2 mg/ml polymer concentration and confirm that the morphologies found by TEM actually exist in solution. Adapted with permission from [176]. Copyright (2008) American Chemical Society.

technique is relevant and could be successfully used for a deeper understanding of conformational changes induced either by dilution or by specific stimuli, such as pH, salt concentration, or temperature [177,178]. For instance, the kinetics of amphiphilic polymers assembly and disassembly in solution can be efficiently monitored using time-resolved cryo-TEM, which allows the real-time observation of nano-systems formation and disruption. Indeed, different stages of micelles development can be studied by analyzing samples that have been vitrified at different time-points from their preparation [72,179,180]. Saito *et al.* [181] evaluated the morphological changes of micelles composed of μ-[PEE][poly(ethylene oxide)][PMCL] (μ-EOC) in an aqueous buffer at pH 12 and 50°C after 2, 7, 14 and 28 days, to determine the impact of alkaline hydrolysis on micelles shape and integrity. Cryo-TEM images showed the transition from cylindrical wormlike

micelles (water, time zero), to sheet-like structures (pH 12, 2 days) and finally to large spherical assembly (pH 12, 14 days) allowing the authors to figure out the mechanisms driving micelles transition.

In addition, Plamper *et al.* [182] illustrated the morphological variations of micelles composed of poly(ethylene oxide) and poly(dimethylaminoethyl methacrylate (PEO_{114}-$(PDMAEMA_{40})_4$-PEO_{114}) when subjected to different temperatures before vitrification. At 70°C, samples appeared as a mixture of spherical micelles and non-spherical aggregates. On the contrary, after vitrification at 40°C, no presence of micelles was registered as only small star-like structures were observed. Finally, at 5°C, another micellization process occurred as testified by cryo-TEM images showing spherical micelles with much bigger dimensions than before. These results confirmed the pivotal role of temperature in driving micellization, influencing size and morphology. Other Authors investigated pH-related morphological changes [126]. Yang *et al.* [183] found spherical micelles of N-dodecyl-1, 4-diaminobutane ($C_{12}N_4N$) at pH 6.99, worm-like micelles at pH 8.27 and a micelle-to-vesicle transition at pH of 9.43, confirming that aggregates morphology varies moving from acidic to basic conditions.

Regarding the impact of salts on micelles structure, Kuperkar *et al.* [184] monitored the effect of $NaNO_3$ on the morphology of hexadecyltrimethylammonium bromide(CTAB) micelles. Briefly, CTAB micellar solutions at concentration of 0.15 M were analyzed at 30°C in absence and presence of increasing salt concentrations. Micelles of CTAB without $NaNO_3$ were spheroidal, as illustrated in Fig. 9A. On the contrary, addition of 0.02 M $NaNO_3$ resulted in a sphere-to-rod transition, and both spheroids and worm-like micelles were found (Fig. 9B). Finally, in the presence of 0.04 M $NaNO_3$.only rod-like structures are present (Fig. 9C).

Ultimately, Cryo-TEM has also been used to evaluate micelle-mucus interaction: Eshel-Green *et al.* [185] prepared indomethacin-loaded micelles of Pluronic®F127 (F127) as well as Pluronic®F127 modified with acrylate end groups (F127DA) in order to increase their mucoadhesive potential. They studied by Cryo-TEM the impact of micelles-mucin interaction on mucin structural features. In absence of the formulation, mucin showed small aggregates with dimension of *approx.* 50 nm. The addition of F127 caused the formation of bigger aggregates (400 nm), and the F127DA/mucin mixture determined a more intense aggregation process producing particles even larger than 400 nm. The microscopy images were supported by DLS and SAXS data to demonstrate the enhanced aggregation in the presence of acrylate end groups.

3.2.4. X-Rays scattering

In recent years, X-ray scattering has been profitably applied to the assessment of the physico-chemical properties of self-assembled colloidal nanosystems intended for drug delivery [186–188]. Among them, polymeric micelles in solution are well suited for being investigated by the non-invasive scattering techniques. These structural studies can help in the selection of the most promising formulations at all stages: preparation, stability and storage, interaction of the nanovectors with model tissues.

In a solution or suspension, micelles scatter a fraction of the incident radiation, according to their concentration, their mass and their contrast against the solvent. The scattered radiation intensity *I(q)* is not uniform in all directions, but it displays a characteristic angular modulation, depending on the ratio between the size of the micelles and the beam wavelength.

For a monodisperse homogeneous micellar solution:

$$I(q) \div c\, M\, (contrast)^2\, P(q)\, S(q)$$

where *c* is the concentration of micelles with mass *M* and *(contrast)* is the contrast of particles, or of regions of the particles, with respect to the solvent. The two modulating terms are expressed as a function of the momentum transfer $q = 2\pi/\lambda\ sin(\theta/2)$, λ being the wavelength of the incident radiation and θ the scattering angle. *P(q)* is the particle form factor, which brings information on the size and shape of the micelles, while *S(q)* is the solution structure factor. *S(q)* depends on the spatial distribution of micelles, becoming constant, $S(q) = 1$, for dilute solutions of non-interacting micelles. This simple general expression for *I(q)* can be completed to describe the scattered radiation from polydisperse systems or from non-homogeneous particles.

X-ray typical wavelength is 0.1 nm and X-ray instruments extend on a wide range of scattering angles from ultrasmall angles (USAXS), small angles (SAXS), and wide angle (WAXS) [189,190] allowing for intensity detection on a wide range of momentum transfer (10^{-3} $nm^{-1} < q < 5\ 10^{1}$ nm^{-1}). The measure of *I(q)* in this wide *q*-range can reveal the structure of the particles from overall shape, *i.e.* μm, to the local details, *i.e.* tenths of nm. Also, it is possible to probe their internal organization, if different portions of the particles have a visibility contrast with each other. The contrast term for X-rays is the difference in the electron density between adjacent regions. This parameter can be calculated for different polymers or surfactants, starting from their chemical formula, that is the number of electrons, and their molecular volume.

3.2.4.1. X-Rays for describing micelles structural parameters. SAXS experiments are extensively applied to investigate the structure of polymeric micelles in solution, empty or loaded with drugs, providing detailed description of their size, shape and inner architecture on the 1-100 nm length-scale [191,192]. The amount of sample needed is tens of μl, in a wide range of concentration, down to few mg/ml, and the acquisition time is very short, from tens of s to tenths of s, depending on the X-ray source.

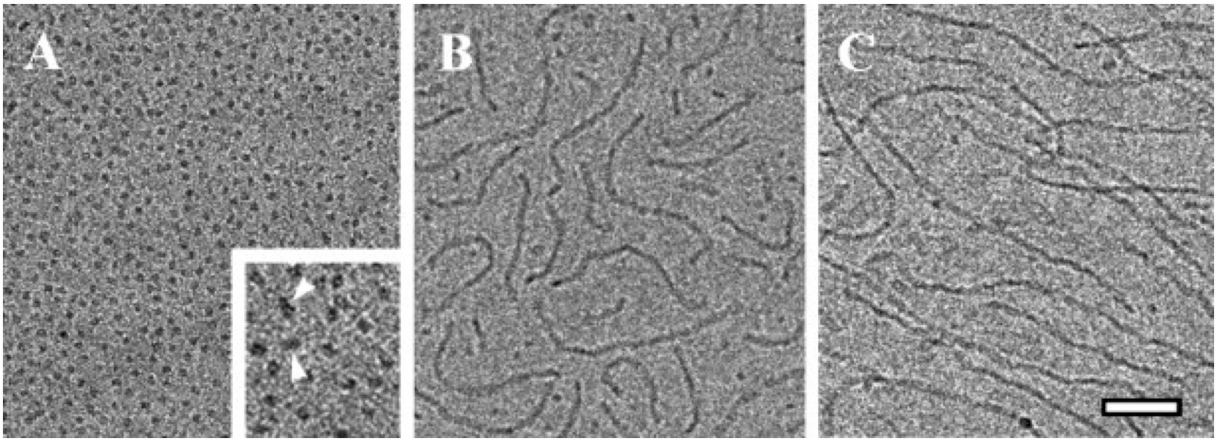

Fig. 9. Cryo-TEM images of 0.15 M CTAB micelles at 30 °C in the absence of $NaNO_3$ (A) and in presence of 0.02 M (B) and of 0.04 M (C) of $NaNO_3$. Scale bar= 50 nm. Reprinted from [184] with permission of Elsevier.

Polymeric micelles can be nanosized spheroids or ellipsoidal objects, rod-like or disk-like, depending on the type of solvent, length of polymer chain, nature and amphiphilic properties of the polymers and temperature [193]. A variety of models for the form factors *P(q)* describing the different polymeric aggregates can be found in the literature, see for example the exhaustive study reported by J. S. Pedersen [194–196].

A core-shell model is often suitable for the description of micelles, where contrast exists between the polymer hydrophobic and hydrophilic components. The core-shell model has been applied to aggregates of linear polymers and block copolymers and of more complex chains, as bottlebrush block copolymers [197].

The size and shape of the micellar core can be derived and the structural changes upon encapsulation of hydrophobic drugs can be assessed. For example, Akiba and coworkers [198] performed SAXS experiments to assess the size of the core of partially benzyl-esterified poly(ethylene glycol)-block-poly(aspartic acid) micelles and to detect its increase from 5.9 to 6.9 nm upon loading with a hydrophobic retinoid antagonist drug (LE540).

The data analysis allowed them to calculate the average number of polymers in each micelle, namely, the aggregation number, that slightly increased from 145 to 182 upon encapsulation of about 8 wt % LE540. Changes in the drug loading were also deduced to affect the size and shape of micelles based on the glycopolymer poly(1-O-methacryloyl-β-D-fructopyranose)-block-poly(methyl methacrylate) (Poly(1-O-MAFru)$_{35}$-b-PMMA$_{145}$), by modelling to a core-shell form factor [199]. Here, the size of the micelles was detected to increase with the amount of loaded paclitaxel, from 26 to 50 nm, reaching the optimal size for cellular endocytosis. Moreover, using SAXS, Authors found that the size of the loaded micelles and the drug location inside the nanovectors depended on the drug-loading method. Particularly, progressive loading of paclitaxel in preformed micelles (two-step process) resulted in drug settling in the outer shell, inducing shell shrinkage and de-hydration, that could explain the observed lower cellular uptake and lower cytotoxicity as compared to the one-step-loaded nanoparticles.

The reconstruction of the architecture of polymeric micelles through the form factor *P(q)* gives information also on the hydrophilic shell thickness and hydration, both in the case of spherical and non-spherical micelles. The shell thickness and the conformation and hydration of the hydrophilic polymer chains have an impact on the fate of the micelle, ranging from its stability in solution to its structural evolution when in interaction with tissues, thus steering the biodistribution and the pharmacokinetics of the drugs. The core-shell-sphere and core-shell-cylinder form factors were applied to model micelles formed by self-assembling of amphiphilic linear diblock copolymers, PEG-*b*-PLA and PEG-*b*-PCL, and heterografted brush copolymer PMGA-g-(PEG/PLA) [200]. Interestingly, the structural parameters (radius and length of cylinders and shell thickness) were further used to calculate the properties of the micellar surface: the number of PEG molecules per interfacial area, and the percent PEG content in the shell. Also, the connection between the structural results on micelles, as determined by SAXS, and their stability and behaviour has been investigated for micelles with various surface PEG densities, revealing a close correlation of surface PEG density with the macrophage uptake and *in vivo* pharmacokinetics [201].

X-ray scattering techniques have been also applied to the investigation of the structure factor *S(q)* that can provide information on the interactions between polymeric micelles or, on a local length-scale, between subregions inside the core of the micelles. Inter-micellar interactions, both attractive and repulsive, impact on the spatial organization of particles in solution [202].

The solution structure factor *S(q)* of interacting micelles has been reported for polymeric micelles, prepared using TPGS (d-α-Tocopheryl polyethylene glycol 1000 succinate), and/or poloxamer 407, as a vehicle for the ocular delivery of lipophilic drugs [121]. From the analysis of the structure factor the characteristic intermicellar distance can be calculated and, given the volume fraction of micelles, the micellar volume and size can be estimated also in concentrated solutions. As micelles are self-aggregating systems, inter-micellar interactions (for example, electrostatic or steric) may impact on their size and shape. The effect of ionic strength, modulating electrostatic repulsion, has been studied on micellar aggregates of oppositely-charged block copolymer polyelectrolytes, following their structural evolution towards the formation, at high ionic strength and temperature, of inverted micelles, where a hydrophobic core and polyelectrolyte shell could be identified [203].

SAXS can be applied also to the characterization of ordered phases, at high concentration, where micelles experience high repulsive interactions and order into liquid crystalline lattices. Thompson and coworkers [204] investigated the cubic structures formed in Pluronics® P104, P105, and F108 solutions at 31% (mass/vol) both neat and co-formulated with the drug cisplatin (0.02% to 0.1%, mass/vol). The phase structure identification, FCC (face-centered cubic) or BCC (body-centered cubic), and the lattice parameter could be identified from the sequence of intensity peaks measured by SAXS.

Complementary wide angle X-ray (WAXS) measurements, acquiring the scattered intensity *I(q)* in the high q region ($10\ nm^{-1} < q < 5\ 10^{1}\ nm^{-1}$), can also be used to provide structural information on the very local length-scale (tenths of nm). Of interest, WAXS experiments can give access to the molecular arrangement within the micellar core, if the hydrophobic moiety packs with a pronounced degree of order at a characteristic distance [205]. WAXS results on the crystal structure of the micellar core has been recently reported by Hayward and coworkers [206] for fiber-like polythiophene block copolymer micelles.

3.2.4.2. X-Rays for monitoring micelles structural evolution and interaction with tissues. The capability of polymeric micelles to interact with different tissues depends on their structural parameters, namely their size, morphology and surface charge, the presence of specific molecules at the surface, and their hydration shell. Often the first tissue that micellar nanovectors encounter is the mucus layer. Mucus permeation, mucoadhesion and cell membrane interaction are key properties for an effective and controlled delivery of drugs through the mucus barrier and inside epithelial cells. The pore size of the mucus mesh limits the size of allowed nanovectors (size-exclusion barrier), while the diverse domains of mucin molecules can interact with both hydrophilic and hydrophobic nanoparticles (interaction barrier) [207].

Several papers report interesting studies on the stability of polymeric micelles in mucus models, and on their ability either to diffuse through artificial/reconstituted mucus layers (mucopenetrating carriers) [65,208] or to be trapped within (muco-adhesive carriers) [26,209–211].

SAXS experiments can provide information on the structural evolution of the nanocarriers when mixed with mucus model, that determines the following drug release behavior. Clementino and coworkers [212] investigated the structural evolution of nanoparticles in mucus upon addition of enzymes that are abundant in nasal secretion. The observed mucus-specific biodegradation process may represent an innovative Trojan-horse strategy, capable of accelerating the release of an encapsulated hydrophobic drug. Also, a novel experimental approach based on SAXS, allowed following the penetration of nanoparticles inside the model mucus matrix. The formulations were put in contact with the mucus model and scattering patterns were acquired at different distances from the interface at different time-delays. Results have been related to the propensity of the formulations to enter the mucus matrix [213].

Moreover, synchrotron X-ray experiments allow to follow the kinetics of micellization by means of time resolved SAXS (Tr-SAXS) in a time window spanning the millisecond to the second range [214]. Using synchrotron small-angle X-ray scattering (Tr-SAXS) integrated with a microfluidic device, micellization kinetics of a diblock co-polymer, poly (ethylene glycol)-b-poly(caprolactone) (PEG-*b*-PCL) was measured *in situ* with temporal resolution of millisecond and spatial resolution of micrometer [215]. The assessment of the kinetics of micellization can

help in the design and optimization of nanoparticle structures and is essential for continuous scalable production of the polymeric micelles, a key parameter in the development of new formulations.

Several conditions can trigger the self-assembly process or induce a stimuli-response in drug loaded micellar systems. In view of this kind of studies and applications, some X-ray synchrotron beamlines have been equipped with stopped-flow rapid mixing devices, allowing for online, easy and controlled change of pH or ionic strength. Also, devices intended for *in situ* rapid pressure and temperature jumps can be mounted on some beamlines, allowing to observe the induced structural transformation of micelles [216].

3.2.5. *Fluorescence-based techniques and Foerster Resonance Energy Transfer (FRET)*

Even if much insight has been gained on micelles' main properties thanks to the techniques listed above, a greater effort should be placed on defining micelles behavior while interacting with biological systems, as this behavior is strongly related to their therapeutic efficacy. Thus, the impact of both physiological and pathological conditions on micelles integrity, target site accumulation, biodistribution and drug release kinetic should be investigated [22,91,217,218]. For studying the interaction between micelles and biological environments, fluorescence techniques are widely used. Several papers describe the labeling of the constitutive unimers and/or the loaded compound with fluorescent dyes followed by sample analysis by confocal microscopy. For instance, Suzuki *et al.* [219] evaluated polymeric micelles distribution in multilayered cell cultures (MCCs) by conjugating the polymer with Cy5-NHS, whereas Valerii *et al.* [220] developed micelles composed of fluorescence-labeled polystyrene-b-poly(methyl acrylate) to describe unimers fate after cellular internalization. Fluorescence-based techniques have been used *in vitro* [220,221], *ex vivo* [222] and *in vivo* [223] to figure out micelles distribution after i.v. injection [224,225] or after oral [226,227] or topical [228] administration. Additionally, the use of organelle-selective dyes can provide information on the intracellular distribution of the compounds [90], even if it is often difficult to figure out the integrity of the micelles and thus the mechanisms of cargo release and cell uptake.

A more sophisticated approach is represented by FRET, a distance-dependent physical process in which non-radiative energy is transferred between two fluorophores, identified as the donor, which is in its excited state, and the acceptor, in its ground-state (Fig. 10A). FRET occurs only if two conditions are respected. The first one is the partial overlap between the emission spectrum of the donor and the excitation spectrum of the acceptor, to produce enough energy for dipole-dipole coupling. The second one is that the two dyes must be in close proximity (distances in the range between 1-10 nm) [91,229]. In these conditions, when the donor is excited, the energy transfer takes place, and is characterized by the quenching of donor fluorescence, the reduction of the fluorescence lifetime and the increase in acceptor fluorescence emission. Thus, by measuring the acceptor fluorescence emission after irradiation with the donor exciting wavelength, information on the proximity of the two dyes can be obtained. Depending on the set-up used (Fig. 11) this technique gives the possibility to study drug release from micelles, micelles kinetic stability in different milieu, micelles integrity in contact with cells and tissue, with the possibility of shedding a light on cellular uptake mechanisms and micelles' in-vivo behavior. The main advantage of FRET is the uniqueness of its chromophores, characterized by very high sensitivity and selectivity. The most common donor/acceptor pairs used for FRET imaging are DiO/DiI, Cy3/Cy5 and Cy5.5/Cy7 [91,136,219,230]; further information on these fluorophores and their main properties can be found in a recent review, together with other possible dye pairs [91]. Limitations of this technique should also be cited: FRET measurements are affected by low signal-to-noise ratio (SNR) resulting in difficulties to distinguish small differences in FRET efficiencies [231]. Additionally, in presence of biological fluids, samples analysis can be affected by some drawbacks

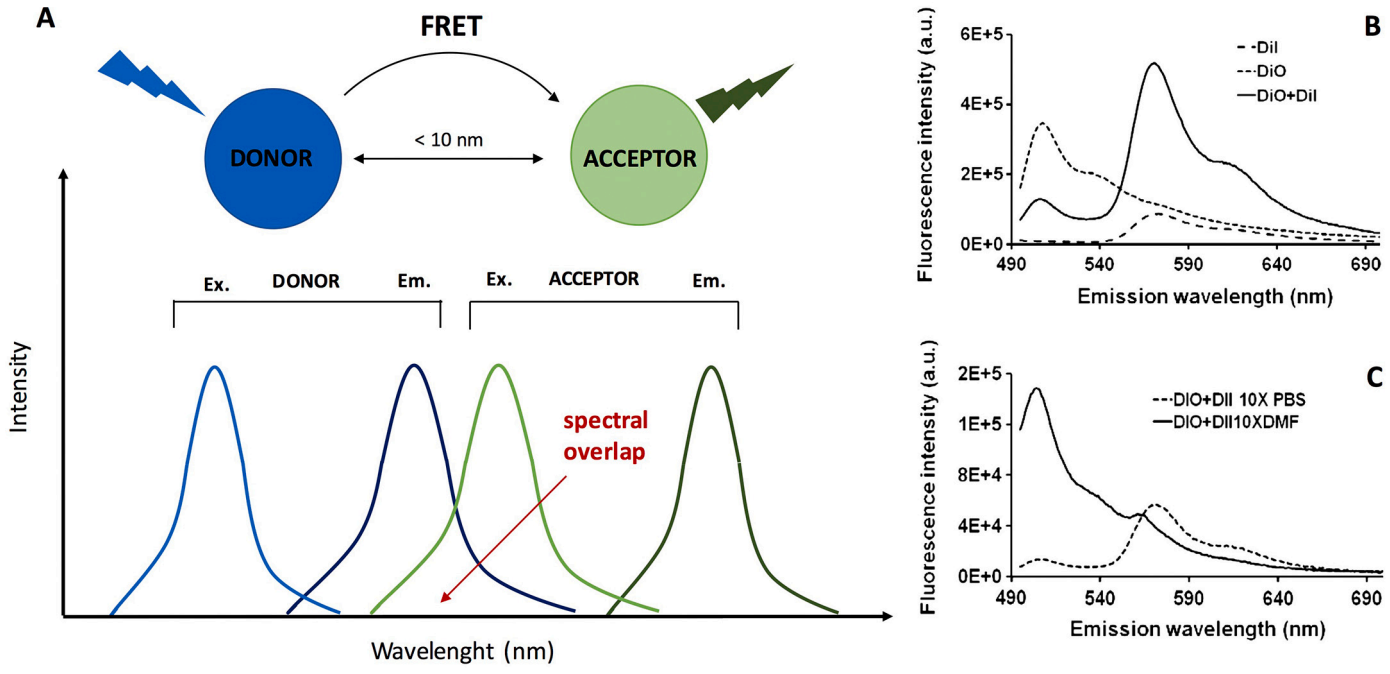

Fig. 10. Panel (A) shows a schematic illustration of FRET, a distance-dependent physical process in which non-radiative energy is transferred between two fluorophores, identified as the donor, which is in its excited state, and the acceptor, found in its ground-state. The spectrum of donor molecule emission (Em.) must be overlapped with the spectrum of acceptor molecule excitation (Ex.). The FRET energy transfer is allowed only when donor and acceptor are found at distances lower than 10 nm. Panel (B) represents FRET signal originated from the analysis of Poly(PS74−b-DMA310) micelles loaded with DiI (donor) alone, DiO (acceptor) alone or co-loaded with DiI and DiO after excitation at 484 nm (DiI excitation wavelength) whereas panel (C) describes the FRET intensity of DiI/DiO-loaded Poly(PS74−b-DMA310) micelles after 10-folds dilution in PBS (intact micelles, FRET on) or DMF (disassembled micelles, no FRET). Panles B and C are reprinted from [136] with permission of Elsevier.

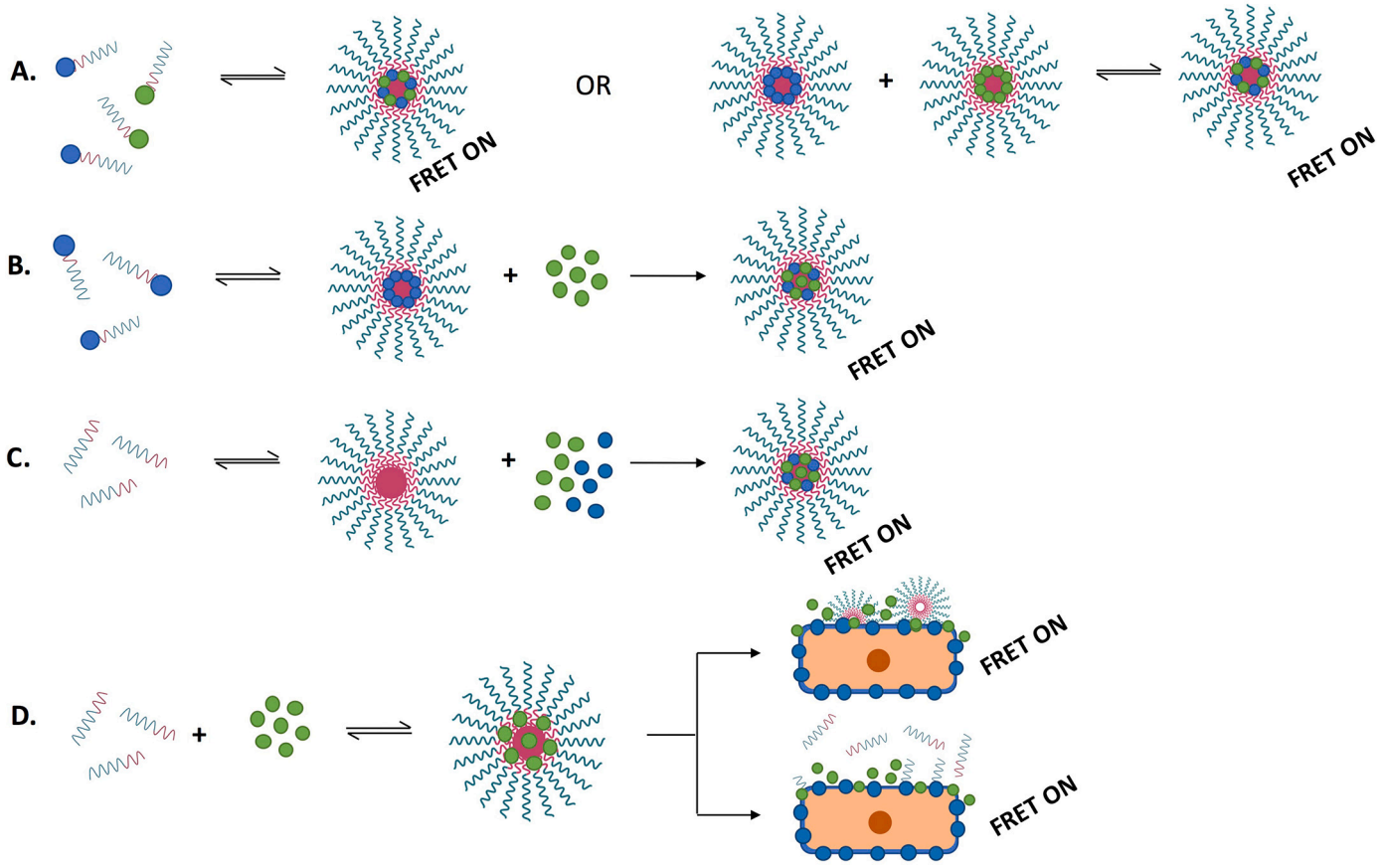

Fig. 11. Different way of micelles labelling with FRET pairs: conjugation of unimers with both donor and acceptor (A); conjugation of unimers with donor/acceptor and loading of the assembled micelles with the acceptor/donor (B); loading of micelles with both donor and acceptor (C); loading of micelles with acceptor and application on cells/tissues that were previously treated with the donor. The donor selectively accumulate in the plasma membrane (D). In case D, FRET signal can be observed only if the acceptor loaded in the micelles is released either from intact micelles or after micelles disaggregation.

since dye pair can co-localize within –for example- lipoproteins, vesicles or other components of the fluids. Finally, the accuracy of the results can be affected by self-quenching phenomena, that can reduce the FRET signal (see par. 3.2.5.3).

3.2.5.1. FRET for micelles static and dynamic characterization. FRET-based strategies have been primary proposed as effective tools for investigating micelles structural characteristics and drug loading (the so-called static characterization), in addition to other properties including their structural stability, environmental responses and drug release kinetics (well-known as dynamic characterization) [91]. By labelling amphiphilic polymers with two different FRET probes, their self-assembling behavior can be assessed through the registration of their energy transfer signal, which takes place if the fluorophores are close to each other (Fig. 11 A). Similarly, it is possible to use a polymer labelled with a probe and verify the FRET signal upon loading the coupled dye (Fig. 11 B). Instead of using modified polymers, another approach is based on the simple loading of micelles with two FRET dyes (donor and acceptor), to observe FRET phenomenon when both probes are entrapped in the micellar core (Fig. 11 C).

Gupta *et al.* [136] evaluated propylene sulfide (PS) and N,N-dimethylacrylamide (DMA) (poly(PS_{74}-b-DMA_{310}) micelles assembly using as FRET dyes DiO and DiI, working respectively as donor and acceptor. As FRET occurs when the two probes are found at distances lower than 10 nm, DiI emission can be detected only as a result of probes co-encapsulation in the nanosystem. On these bases, micelles formation and dye co-encapsulation was demonstrated after registration of an emission spectrum showing a fluorescence peak at the emission wavelength of DiI (Fig. 10B). The emission spectra obtained after 10-fold dilution either with PBS or with dimethylformamide (DMF) confirmed the effectiveness of the technique in demonstrating micelle integrity (PBS) or disassembly (DMF) (Fig. 10C).

FRET can also be used for the dynamic characterization of the micelles by monitoring the exchange of loaded molecule between two micelle populations [232]. In this case, two different populations of micelles are prepared: one loaded only with the donor, and the other loaded only with the acceptor. By mixing the two populations and recording the emission spectra as a function of time, information on exchange dynamics can be obtained (Fig. 11A). Indeed, if the dye is stably encapsulated, no FRET will be observed since the distance between the two fluorophores is higher than the Föerster radius. On the contrary, if the equilibration will cause acceptor and donor to occupy the same micelles an increased FRET signal will be recorded. With this technique, Jiwpanich *et al.* [232] demonstrated significant differences in the stability of micelles depending on the composition (for instance tween 80 and CTAB *vs* poloxamers) and also evaluated the role of the cross-linking in tuning the rate of exchange.

FRET can be an appropriate method also for investigating micelles stability in fluids mimicking biological conditions to better predict micelles tendency to disaggregate when administered *in vivo*. For instance, Lu *et al.* [233] prepared DiO/DiI-loaded polymeric micelles and evaluated the drug release after incubation with FBS at 37°C for 48h. An increase in the fluorescence intensity at 501 nm and a decrease at 565 nm over time indicated probes slow release from micelles probably due to their disassembly. This technique allowed for the estimation of the approximate micelles half-life in serum (9 hours), suggesting their

potential as drug carriers for intravenous infusion.

Despite the interest of this technique in the evaluation of the dynamic of polymeric micelles, it is important to underline that the behavior of the dye will not necessarily reflect the behavior of an encapsulated drug. Indeed, specific and molecule-dependent interactions take place between the cargo and the micellar core.

3.2.5.2. Investigation of micelles-cells interaction by FRET. Micelle-cell interaction can remarkably affect micelles stability and drug release and FRET can be used to shed a light on this topic [91,92,218]. Xiao *et al.* [162] used FRET to evaluate if PEG-*b*-PLA micelles entered intact inside human ovarian cells or released their cargo on the plasma membrane. 5-dodecanoylaminofluorescein (DAF), characterized by the ability to accumulate in cellular membranes, was used as donor, whereas Nile-Red (NR) was chosen as acceptor and loaded in the micellar core (Fig. 11D). Cells were treated with DAF, with NR-loaded micelles (M-NR) or with the combination of the two. FRET could not be observed in case of DAF and NR alone, while an increased FRET signal in the cellular membrane was detected after treatment with both, indicating NR and DAF co-localization. Moreover, this result demonstrated NR release from the micelles, since FRET cannot occur when the compound is still incorporated in the micellar core because, in this case, the distance between DAF and NR is too far. Another study was carried out by Lee *et al.* [92] in order to investigate the impact of micelles' stability in cellular internalization pathway. With this aim, they compared self-assembled micelles made of mPEG-PDLLA with micelles stabilized by disulfide bonds and made by mPEG-(Cys)4-PDLLA. Different types of cancer cells (human breast, mouse lung and human prostate) were incubated for 2 h with DiO and DiI-loaded micelles and FRET signal was measured after excitation at 488 nm. The resulting images (Fig. 12) highlight the presence of FRET signal outside the cells for both type of micelles, an intense green fluorescence (due to DiO emission) in the plasma membrane only in the case of mPEG-PDLLA micelles, and for both mPEG-PDLLA and disulfide bonded micelles a yellow fluorescence inside cells, originated from the overlap between red (DiI) and green signal (DiO), that testify the presence of both probes at a distance longer than Föerster radius (no FRET). Thanks to these results, integrated with data on endocytic trafficking, different drug delivery mechanisms have been demonstrated: self-assembled micelles (mPEG-PDLLA), that are intact in the extracellular space, dissociated following micelle–membrane interactions, and the hydrophobic probe (DiO) accumulated in the plasma membrane. Alternatively, disulfide bonded micelles (mPEG-(Cys)4-PDLLA) were internalized via endocytic pathways and then decomposed in endosomes, probably caused by the intervention of reducing agents.

Other authors studied [234] the intracellular fate of micelles containing a fluorescently labeled copolymer (FITC labelled PEG-PDLLA) and a hydrophobic fluorescent probe (Dil). The results highlighted that cellular uptake of the probe was much faster than that of the labeled copolymers, indicating that the hydrophobic probe in the core was released from micelles in the extracellular space. Additionally, by loading both DiO and Dil, it was possible to confirm by FRET that the two dyes were first released to plasma membranes and then entered the cells afterward; indeed a high FRET signal was observed outside the cells, while a low FRET was observed on membrane and inside the cells.

3.2.5.3. In vivo real-time FRET for describing micelles stability in plasma. In case of i.v. administration, micellar integrity is an important requisite for efficient drug transport and delivery; shear stress due to the injection as well as the contact with plasma components can interfere with micelle assembly. Morton *et al.* [230] used *in vivo* real time FRET in a mouse model, to monitor both micelles disassembly in the bloodstream and drug-micelles dissociation. To investigate the release of the cargo from

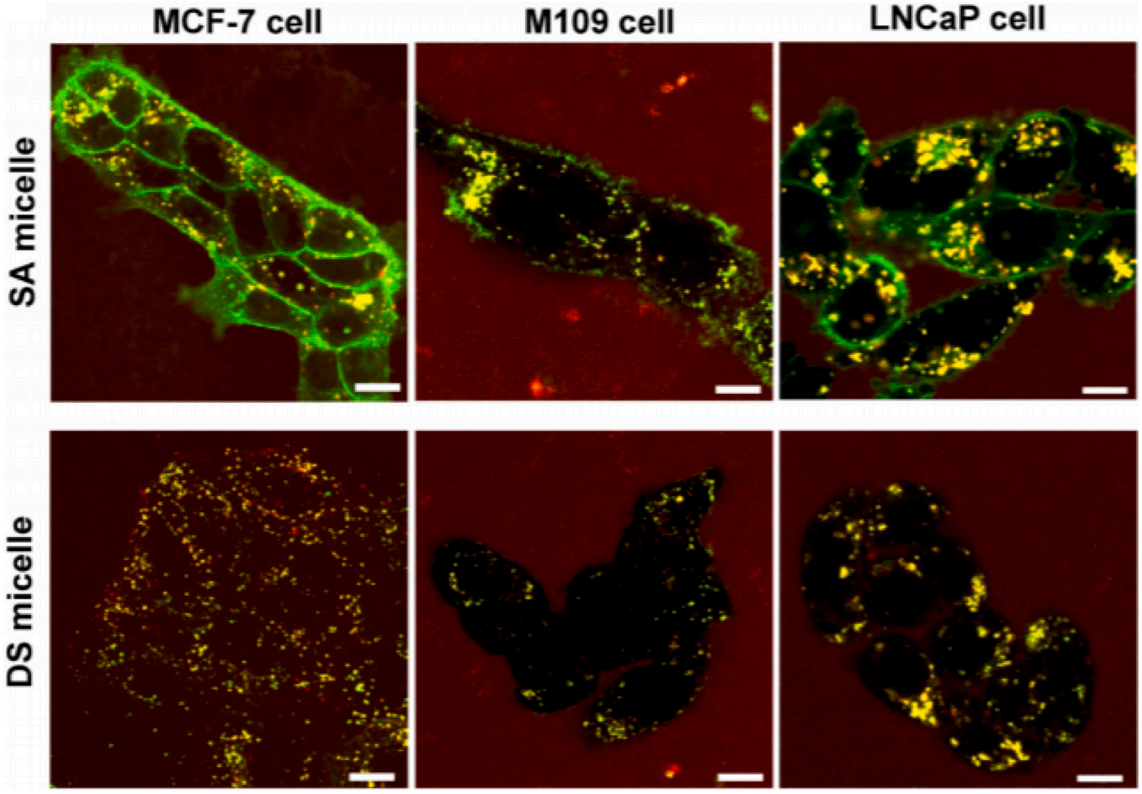

Fig. 12. Different cellular internalizations of self-assembled and disulfide bonded micelles. Confocal FRET images of MCF7, M109, and LNCaP cells after 2 h incubation with self-assembled and disulfide-bonded FRET micelles. The green color represent DiO signal. Red fluorescence indicate FRET (Dil emission) while the yellow color indicates overlapped signals of the two dyes (absence of FRET). The concentration of each FRET micelle was 500 μg/mL, and the excitation wavelength was 488 nm. (Scale bars: 10 μm.) Adapted with permission from [92]. Copyright (2013) American Chemical Society.

micelles, the polymer (PEG-*b*-PPLG) was derivatized with a fluorescent probe (Cy7, acceptor) and the micelle was loaded with a small molecule dye (Cy5.5, donor) (as in Fig. 11B). To investigate micelles disassembly, blank micelles were formulated using both PEG-*b*-PPLG-Cy5.5 and PEG-*b*-PPLG-Cy7 (as in Fig. 11B). The data highlighted that blank micelles are stable up to 72 h (FRET efficiency between 50 and 85%), while the incorporation of the dye brought to a significant and rapid reduction of FRET efficiency, indicating a significant impact of the cargo on micelles stability and/or a rapid dye release. It is however important to underline that the behavior of the dye will not necessarily reflect the behavior of an encapsulated drug. Indeed, specific and molecule-dependent interactions take place between the cargo and the micellar core. The low stability of micelles in plasma is also supported by the data previously published by Chen et *al.* [235], focused on poly(ethylene glycol)-poly(d,l-lactic acid) (PEG-PDLLA) micelles. Blood vessel in the ear lobes were visualized *via* real-time FRET after intravenous injection of DiO/DiI-loaded micelles through tail veins of a mouse. As showed in Fig. 13A, emission signals of the two FRET probes were registered after 15 min, 1 h and 3 h. The spectra recorded (Fig. 13B) showed a peak with increasing intensity around 501 nm caused by DiO emission and a peak with decreasing intensity at higher wavelengths originated from DiI emission (FRET), indicating the quick release of the compounds from the micellar core.

Using *in vivo* real time FRET, Sun *et al.* [236] studied micelles clearance, describing how quickly and by what mechanism polymeric micelles are eliminated. FRET-imaging (covalently bound dyes: Cy5 and Cy5.5) in a mice model bearing subcutaneous HepG2 tumor highlighted that in blood vessels the 80% of injected micelles made either of poly-ethylene glycol-block-poly(ε-caprolactone) (PEG-PCL) or PEG-block-poly(d,l-lactide) (PEG-PDLLA) quickly dissociate into unimers, while the remaining micelles (20%), penetrate, intact, the tumoral tissue. Still on PEG-PCL micelles, different results were very recently obtained by Zhang *et al.* [237] which reported that approximately 60% of PEG-PCL micelles in mouse plasma were intact 72 h after i.v. injection, *i.e.* most of micelles remain intact during blood circulation. The discrepancies with respect to other published papers (see above) are attributed to differences in the fluorophores used that, if characterized by a large Stokes shift, minimize the self-quenching effect enhancing the accuracy of the results. Indeed, the limiting step of FRET consists in the possible self-quenching of fluorophores which, if ignored, can lead to a mistaken data interpretation. Additionally, authors provided a mathematical formula for calculating micellar integrity in order to obtain an accurate quantification via the combination of spectral analysis and mathematical derivation [237].

3.2.6. *Separation techniques for micelles stability evaluation*

To study micelles stability, other techniques have also been evaluated. Gel permeation chromatography, and in general size exclusion chromatography, can be used to separate intact micelles from unimers since, due to the different size, they will have different elution volumes/times. These techniques has been used to differentiate between encapsulated and non-encapsulated drug [238] and, in combination with other techniques, to evaluate the integrity of micelles in plasma [239]. The technique presents several limitations, since strong interactions can take place between micelles and stationary phase, with possible irreversible adsorption, micelles disaggregation, or column clogging.

Asymmetrical flow field-flow fractionation (AF4) is a flow fractionation technique that separates nano-sized solutes based on their

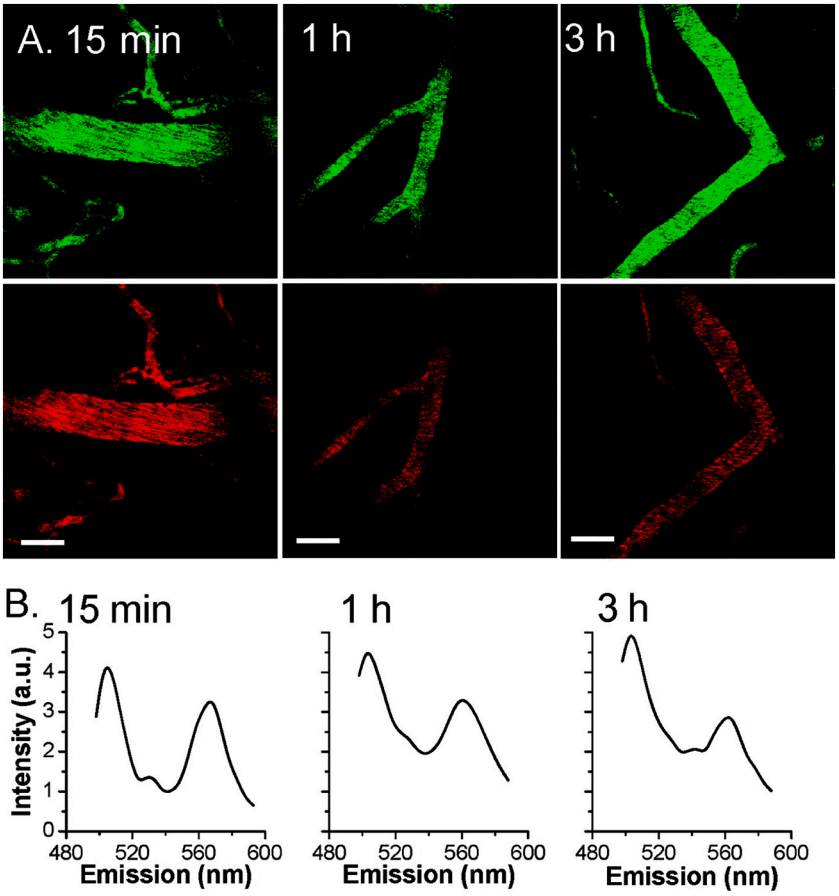

Fig. 13. *In vivo* imaging of FRET micelles intravenously injected into a mouse through the tail vein. The fluorescence signals were measured after 15 min, 1h and 3 h from the injection. (A) DiO (green) and DiI (red, FRET) signals observed in blood vessels. Bar = 50 μm. (B) Fluorescence spectra in blood vessels. Adapted with permission from [235]. Copyright (2008) American Chemical Society.

hydrodynamic size in an open channel by applying a cross-flow through an ultrafiltration membrane. Typically, in the field of nanomedicine, AF4 is coupled with detectors such as ultraviolet-visible or fluorescence, refractive index (RI) or dynamic light scattering (DLS) [240]. Its more interesting application concerns the study of micelles stability in complex biological matrices [241], since it is possible to separate intact micelles from unimers and from biological fluid components, without the inconveniencies of the chromatographic techniques. Very recently, the data obtained with AF4 in terms of micelles integrity have been correlated with the pharmacokinetic profile, allowing to predict the stability or instability of drug loaded micelles after i.v. administration [242].

Density gradient ultracentrifugation is a promising approach for separating complexes such as acellular biologic macromolecules, synthetic nanoparticles and cellular components on the basis of their molecular masses [243]. Two different ultracentrifugation technique have been described in literature. The first one, known as zonal centrifugation, is based on a preformed gradient causing particles sedimentation as band or zone at a rate dependent on their size, shape and density. As in this case centrifugation stops when a sufficient separation of the desired compounds is achieved, the run is interrupted while sedimentation is still ongoing [244]. The second strategy, defined as isopycnic centrifugation, leads to micelles separation according to their density, as their size affects solely the rate at which sedimentation is reached. In other words, particles move until reaching their isopycnic points, representing the point at which their density is the same as the one of the surrounding environment [245,246]. In contrast with zonal centrifugation, isopycnic centrifugation can be performed using both preformed and self-forming gradients [246]. The most common application of density ultracentrifugation has been indicated in the separation and purification of various nanoparticles in order to successfully obtain monodispersed colloidal nanosystems in aqueous as well as organic phase [247]. Recently, this technique has been used for the study of micelles disaggregation tendency in biological fluids, providing a detailed representation of micelles behavior in biorelevant conditions. Langridge *et al.* [243] have associated FRET with density ultracentrifugation to assess the effect of different biological fluids (namely, cerebrospinal fluid, ascites fluid, serum, pleural fluid and synovial fluid) on micelles stability. They mixed the micelles (loaded with a fluorescent probe) either with PBS or with the different biological fluids, then applied the obtained mixture to a sucrose gradient and ultracentrifuged for 24 h. The fluorescence path obtained in PBS was considered as a "reference" indicating the position of intact micelles in the gradient. A transfer of fluorescence to less dense fractions highlighted the dissociation of the micelle cargo within the body fluid. On the contrary, the sedimentation into more dense layers suggested that the micelles may be associated with body fluid components. Thanks to this technique, it was possible to describe micelles stability as a function of the block-copolymer used and to identify the role of the different body fluids. Overall, the data confirmed the higher stability of micelles characterized by longer hydrophobic blocks, but also indicated that, in complex biologic fluids, CMC values are not always predictive of micelle stability. Additionally, micelles disassembling depended upon fluid identity; the simple protein content of the fluid was not predictive of the fluid disrupting capability, while, in general, the lipid content did correlate with cargo extraction and, possibly, with micelles disassembly.

4. Regulatory aspects and concluding remarks

Regulation on the pharmaceutical development of a new formulation is contained in ICH Pharmaceutical Development Q8(R2) guideline. Due to their nano-scale size, polymeric micelles should undergo further specific requirements in order to ensure safety of products avoiding risks related to unpredicted effects on patients [248,249]. Beyond the requirements concerning all nanocarriers, due to their peculiarity, their extensive assessment, with in-depth characterization and understanding of crucial properties, is addressed in a specific EMA Reflection Paper published in 2013 on the development of block copolymer micelle medicinal products [27].

The document provides basic information for the quality characterization, product specification, stability, manufacturing, non-clinical pharmacokinetics (PK) and pharmacodynamics (PD) studies as well as some considerations for first-in-human studies. The paper is mainly focused on products for intravenous administration, however it is clearly indicated that the principles outlined can also be applicable to other routes of administration. Together with the physicochemical evaluation of polymers and active substances (chemical stability and impurity profile), the document suggests the evaluation of CMC, micelles size, morphology, surface charge, stability in plasma or other relevant media and drug release in biorelevant conditions. The main features dealt with in the reflection paper have been summarized in Fig. 14. From this scheme, it is evident that micelle's characterization represents the fundamental basis to set-up product specifications and stability studies but also to design pharmacokinetics and pharmacodynamics studies. For instance, the sampling schedule for PK studies should be selected considering micelles stability; analogously, PD studies should be designed taking into account the fate of the drug (i.e. the site and rate of release) as well as the fate of the micelles following administration and/or cellular entry. The lack of compendial (pharmacopoeia) methods for the evaluation of drug release and micelles integrity makes it necessary to set-up in-house methods that must be validated not only regarding reproducibility, but also in relation to their discriminating power. These validated tests, to be applied routinely to the micellar formulation, should be able to predict the release when in the circulation and/or at the targeted site of action, thus the proposed release media should reflect the physiological environment of micelle when in use. On the other side, the method should also be sensitive enough to ensure batch-to-batch consistency. The complexity of the micellar systems and the challenges related to their characterization need an early dialogue with the regulators to discuss both the critical product attributes and emerging methods that might be applied to define and characterize these formulations in vitro and in vivo. The predictivity of the in vitro tests is however a critical issue and even in the reflection paper it is acknowledged that it may not always be possible to establish in vitro-in vivo correlations. At the moment, very few papers addressing the correlation between in vitro drug release (and/or micelle stability) and drug pharmacokinetics are present in the literature: Zhang *et al.* [237] performed in vitro experiments of PEG-PCL micelles stability using mouse serum and found a reasonable agreement with in vivo data: after 72 h, 70% of the micelles were intact in the in vitro experiment, versus 60% found in vivo in the bloodstream. Liu *et al.* [127] studied the interactions between micelles and different plasma proteins by using AF4 coupled with fluorescence and DLS and obtained strong indications for their stability or instability in vivo. Indeed, the behavior of micelles in vivo in the bloodstream resulted very well in line with the in vitro stability. It is, however, important to underline that generalization is not possible: very recently, Bagheri *et al.* [250] by using similar techniques studied the fate of curcumin-loaded polymeric micelles. They found an agreement between micelles circulation time and AF4 in vitro data in plasma, but a faster clearance of curcumin in vivo compared to in vitro studies. This result, attributed to the interaction of curcumin with blood cells, suggests that the characteristics of the polymer and of the loaded drug can highly impact the method predictivity, and indicates that, in the perspective of future development, the set-up of the method should always be drug and formulation –specific.

The stability and the need for a specific characterization represent the two most important obstacles to the clinical development of polymeric micelles. Addressing these issues through the development and validation of specific methods could help to reduce the gap between the academic research field (where micelles are intensively and successfully studied) and formulation development, accelerating their clinical translation.

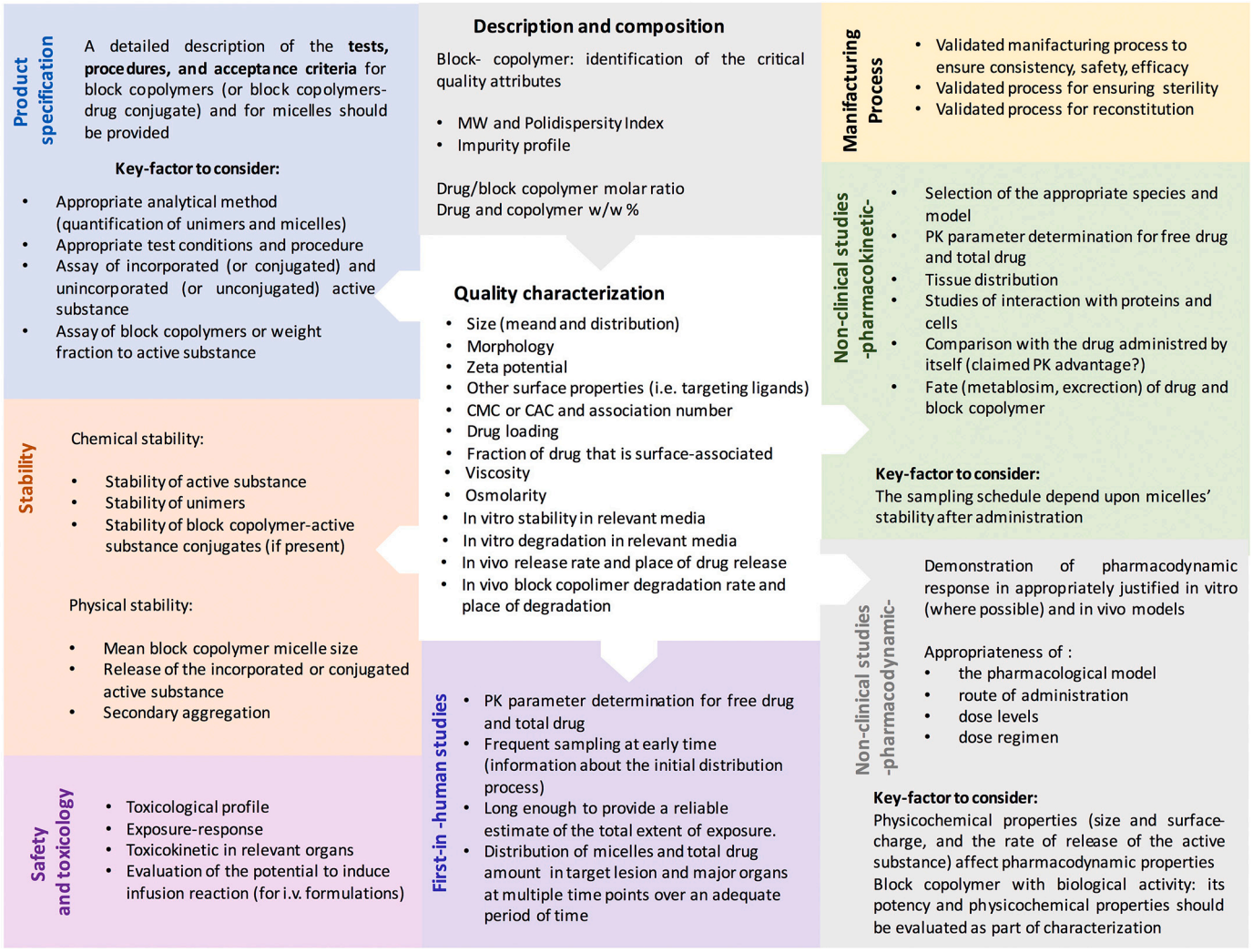

Fig. 14. Summary of various features addressed in the EMA reflection paper on polymeric micelles.

Funding

This work was supported by a Grant from the Italian Ministry of Research (Grant PRIN 2017 # 20173ZECCM Tackling biological barriers to antigen delivery by nanotechnological vaccines (NanoTechVax).

Declaration of Competing Interest

The authors report no conflicts of interest.

References

[1] Z. Chen, Small-molecule delivery by nanoparticles for anticancer therapy, Trends Mol. Med. 16 (2010) 594–602.
[2] B. Salehi, D. Calina, A.O. Docea, N. Koirala, S. Aryal, D. Lombardo, L. Pasqua, Y. Taheri, C.M.S. Castillo, M. Martorell, N. Martins, M. Iriti, H.A.R. Suleria, J. Sharifi-Rad, Curcumin's nanomedicine formulations for therapeutic application in neurological diseases, J. Clin. Med. 9 (2020).
[3] C. Caddeo, M. Manconi, A.M. Fadda, F. Lai, S. Lampis, O. Diez-Sales, C. Sinico, Nanocarriers for antioxidant resveratrol: Formulation approach, vesicle self-assembly and stability evaluation, Colloids Surf. B: Biointerfaces 111 (2013) 327–332.
[4] A. Kumar, A. Ahuja, J. Ali, S. Baboota, Curcumin-loaded lipid nanocarrier for improving bioavailability, stability and cytotoxicity against malignant glioma cells, Drug Delivery 23 (2016) 214–229.
[5] D.J. Irvine, E.L. Dane, Enhancing cancer immunotherapy with nanomedicine, Nat. Rev. Immunol. 20 (2020) 321–334.
[6] J.K. Patra, G. Das, L.F. Fraceto, E.V.R. Campos, M.D.P. Rodriguez-Torres, L. S. Acosta-Torres, L.A. Diaz-Torres, R. Grillo, M.K. Swamy, S. Sharma, S. Habtemariam, H.-S. Shin, Nano based drug delivery systems: recent developments and future prospects, J. Nanobiotechnol. 16 (2018) 71.
[7] Y. Shi, R. van der Meel, X. Chen, T. Lammers, The EPR effect and beyond: Strategies to improve tumor targeting and cancer nanomedicine treatment efficacy, Theranostics 10 (2020) 7921–7924.
[8] J.L. Paris, M. Vallet-Regí, Ultrasound-Activated Nanomaterials for Therapeutics, Bull. Chem. Soc. Jpn. 93 (2019) 220–229.
[9] S.S. Das, P. Bharadwaj, M. Bilal, M. Barani, A. Rahdar, P. Taboada, S. Bungau, G. Z. Kyzas, Stimuli-responsive polymeric nanocarriers for drug delivery, imaging, and theragnosis, Polymers 12 (2020) 1397.
[10] K.V. Jaspreet, K.R. Maram, D.L. Vinod, Nanosystems in drug targeting: opportunities and challenges, Curr. Nanosci. 1 (2005) 47–64.
[11] S. Eom, G. Choi, H. Nakamura, J.-H. Choy, 2-Dimensional Nanomaterials with Imaging and Diagnostic Functions for Nanomedicine; A Review, Bull. Chem. Soc. Jpn. 93 (2019) 1–12.
[12] C. Domingues, C. Alvarez-Lorenzo, A. Concheiro, F. Veiga, A. Figueiras, Nanotheranostic Pluronic-Like Polymeric Micelles: Shedding Light into the Dark Shadows of Tumors, Mol. Pharm. 16 (2019) 4757–4774.
[13] Y. Eygeris, S. Patel, A. Jozic, G. Sahay, Deconvoluting Lipid Nanoparticle Structure for Messenger RNA Delivery, Nano Lett. 20 (2020) 4543–4549.
[14] CHMP, Comirnaty - Assessment Report, 2020.
[15] CHMP, COVID-19 Vaccine Moderna - Assessment Report, 2021.
[16] V. Gadekar, Y. Borade, S. Kannaujia, K. Rajpoot, N. Anup, V. Tambe, K. Kalia, R. K. Tekade, Nanomedicines accessible in the market for clinical interventions, J. Control. Release 330 (2021) 372–397.
[17] D.J.A. Crommelin, P. van Hoogevest, G. Storm, The role of liposomes in clinical nanomedicine development. What now? Now what? J. Control. Release 318 (2020) 256–263.
[18] Y. Zhang, Y. Huang, S. Li, Polymeric micelles: nanocarriers for cancer-targeted drug delivery, AAPS PharmSciTech 15 (2014) 862–871.
[19] Y. Lu, E. Zhang, J. Yang, Z. Cao, Strategies to improve micelle stability for drug delivery, Nano Res. 11 (2018) 4985–4998.

[20] M. Yousefpour Marzbali, A. Yari Khosroushahi, Polymeric micelles as mighty nanocarriers for cancer gene therapy: a review, Cancer Chemother. Pharmacol. 79 (2017) 637–649.
[21] R. Paliwal, R.J. Babu, S. Palakurthi, Nanomedicine scale-up technologies: feasibilities and challenges, AAPS PharmSciTech 15 (2014) 1527–1534.
[22] S.C. Owen, D.P.Y. Chan, M.S. Shoichet, Polymeric micelle stability, Nano Today 7 (2012) 53–65.
[23] I. Pepić, J. Lovrić, J. Filipović-Grčić, How do polymeric micelles cross epithelial barriers? Eur. J. Pharm. Sci. 50 (2013) 42–55.
[24] L. Houdaihed, J.C. Evans, C. Allen, Overcoming the road blocks: advancement of block copolymer micelles for cancer therapy in the clinic, Mol. Pharm. 14 (2017) 2503–2517.
[25] M. Cagel, F.C. Tesan, E. Bernabeu, M.J. Salgueiro, M.B. Zubillaga, M.A. Moretton, D.A. Chiappetta, Polymeric mixed micelles as nanomedicines: Achievements and perspectives, Eur. J. Pharm. Biopharm. 113 (2017) 211–228.
[26] Polymeric Micelles in Mucosal Drug Delivery, Challenges towards clinical translation, Biotechnol. Adv. 33 (2015) 1380–1392.
[27] CHMP, Joint MHLW/EMA Reflection Paper on the Development of Block Copolymer Micelle Medicinal Products, 2013.
[28] H.K.S. Yadav, A.A. Almokdad, S.I.M. Shaluf, M.S. Debe, Chapter 17 - polymer-based nanomaterials for drug-delivery carriers, in: S.S. Mohapatra, S. Ranjan, N. Dasgupta, R.K. Mishra, S. Thomas (Eds.), Nanocarriers for Drug Delivery, Elsevier, 2019, pp. 531–556.
[29] A. Fluksman, B. Ofra, A robust method for critical micelle concentration determination using coumarin-6 as a fluorescent probe, Anal. Methods 11 (2019).
[30] A.N. Martin, Y. Singh, Martin's physical pharmacy and pharmaceutical sciences: physical chemical and biopharmaceutical principles in the pharmaceutical sciences, 2011.
[31] Y. Lu, K. Park, Polymeric micelles and alternative nanonized delivery vehicles for poorly soluble drugs, Int. J. Pharm. 453 (2013) 198–214.
[32] Stability Issues of Polymeric Micelles, J. Control. Release 131 (2008) 2–4.
[33] R. Trivedi, U.B. Kompella, Nanomicellar formulations for sustained drug delivery: strategies and underlying principles, Nanomedicine 5 (2010) 485–505.
[34] R. Wakaskar, Polymeric micelles and their properties, J. Nanomed. Nanotechnol. 08 (2017).
[35] Application of solid phase peptide synthesis to engineering PEO–peptide block copolymers for drug delivery, Colloids Surf. B: Biointerfaces 30 (2003) 323–334.
[36] Polymeric micelles for ocular drug delivery: From structural frameworks to recent preclinical studies, J. Control. Release 248 (2017) 96–116.
[37] S.S. Kulthe, Y.M. Choudhari, N.N. Inamdar, V. Mourya, Polymeric micelles: authoritative aspects for drug delivery, Des. Monomers Polym. 15 (5) (2012) 465–521.
[38] G.B. Jiang, D. Quan, K. Liao, H. Wang, Preparation of polymeric micelles based on chitosan bearing a small amount of highly hydrophobic groups, Carbohydr. Polym. 66 (2006) 514–520.
[39] J. Li, Z. Li, T. Zhou, J. Zhang, H. Xia, H. Li, J. He, S. He, L. Wang, Positively charged micelles based on a triblock copolymer demonstrate enhanced corneal penetration, Int. J. Nanomedicine 10 (2015) 6027.
[40] Micellar carriers for the delivery of multiple therapeutic agents, Colloids Surf. B: Biointerfaces 135 (2015) 291–308.
[41] H.M. Aliabadi, A. Lavasanifar, Polymeric micelles for drug delivery, Expert Opinion on Drug Delivery 3 (2006) 139–162.
[42] B.S. Makhmalzade, F. Chavoshy, Polymeric micelles as cutaneous drug delivery system in normal skin and dermatological disorders, J. Adv. Pharm. Tech Res. 9 (2018) 2–8.
[43] G. Gaucher, M.-H. Dufresne, V.P. Sant, N. Kang, D. Maysinger, J.-C. Leroux, Block copolymer micelles: preparation, characterization and application in drug delivery, J. Control. Release 109 (2005) 169–188.
[44] D.J. Shaw, Introduction to Colloid and Surface Chemistry, Elsevier, 2013.
[45] A.V. Ambade, E.N. Savariar, S. Thayumanavan, Dendrimeric micelles for controlled drug release and targeted delivery, Mol. Pharm. 2 (2005) 264–272.
[46] A.S. Mikhail, C. Allen, Block copolymer micelles for delivery of cancer therapy: Transport at the whole body, tissue and cellular levels, J. Control. Release 138 (2009) 214–223.
[47] H. Cho, T.C. Lai, K. Tomoda, G.S. Kwon, Polymeric Micelles for Multi-Drug Delivery in Cancer, AAPS PharmSciTech 16 (2015) 10–20.
[48] S. Sally, A. Mona, A. Mahmoud, M. Moustafa Taha, A. Doaa, M. Rania, K. Sherine, B. Adnan, E. Kadria, E. May Freag Ahmed, Self-assembled nanocarriers based on amphiphilic natural polymers for anti- cancer drug delivery applications, Curr. Pharm. Des. 23 (2017) 5213–5229.
[49] M. Jones, J. Leroux, Polymeric micelles - a new generation of colloidal drug carriers 48, Eur. J. Pharm. Biopharm, 1999, pp. 101–111.
[50] G. Gaucher, P. Satturwar, M.-C. Jones, A. Furtos, J.-C. Leroux, Polymeric micelles for oral drug delivery, Eur. J. Pharm. Biopharm. 76 (2010) 147–158.
[51] A.R. Khan, M. Liu, M.W. Khan, G. Zhai, Progress in brain targeting drug delivery system by nasal route, J. Control. Release 268 (2017) 364–389.
[52] M.A. Grimaudo, S. Pescina, C. Padula, P. Santi, A. Concheiro, C. Alvarez-Lorenzo, S. Nicoli, Topical application of polymeric nanomicelles in ophthalmology: a review on research efforts for the noninvasive delivery of ocular therapeutics, Expert Opinion on Drug Delivery 16 (2019) 397–413.
[53] X. Duan, Y. Li, Physicochemical characteristics of nanoparticles affect circulation, biodistribution, cellular internalization, and trafficking, Small (Weinheim an der Bergstrasse, Germany) 9 (2013).
[54] N. Hoshyar, S. Gray, H. Han, G. Bao, The effect of nanoparticle size on in vivo pharmacokinetics and cellular interaction, Nanomedicine 11 (2016) 673–692.
[55] J. Yue, S. Liu, Z. Xie, Y. Xing, X. Jing, Size-dependent biodistribution and antitumor efficacy of polymer micelle drug delivery systems, J. Mater. Chem. B 2013 (2013).
[56] J. Wang, W. Mao, L.L. Lock, J. Tang, M. Sui, W. Sun, H. Cui, D. Xu, Y. Shen, The role of micelle size in tumor accumulation, penetration, and treatment, ACS Nano 9 (2015) 7195–7206.
[57] H. Cabral, Y. Matsumoto, K. Mizuno, Q. Chen, M. Murakami, M. Kimura, Y. Terada, M.R. Kano, K. Miyazono, M. Uesaka, N. Nishiyama, K. Kataoka, Accumulation of sub-100 nm polymeric micelles in poorly permeable tumours depends on size, Nat. Nanotechnol. 6 (2011) 815–823.
[58] X. Murgia, P. Pawelzyk, U.F. Schaefer, C. Wagner, N. Willenbacher, C.-M. Lehr, Size-Limited Penetration of Nanoparticles into Porcine Respiratory Mucus after Aerosol Deposition, Biomacromolecules 17 (2016) 1536–1542.
[59] S. Rossi, B. Vigani, G. Sandri, M.C. Bonferoni, C.M. Caramella, F. Ferrari, Recent advances in the mucus-interacting approach for vaginal drug delivery: from mucoadhesive to mucus-penetrating nanoparticles 16, Expert Opinion On Drug Delivery, 2019, pp. 777–781.
[60] S. Salatin, S. Maleki Dizaj, A. Yari Khosroushahi, Effect of the surface modification, size, and shape on cellular uptake of nanoparticles, Cell Biol. Int. 39 (2015) 881–890.
[61] D. Vllasaliu, R. Fowler, S. Stolnik, PEGylated nanomedicines: recent progress and remaining concerns, Expert Opinion on Drug Delivery 11 (2014) 139–154.
[62] J. Logie, S.C. Owen, C.K. McLaughlin, M.S. Shoichet, PEG-Graft Density Controls Polymeric Nanoparticle Micelle Stability, Chem. Mater. 26 (2014) 2847–2855.
[63] Y. Zhu, T. Meng, Y. Tan, X. Yang, Y. Liu, X. Liu, F. Yu, L. Wen, S. Dai, H. Yuan, F. Hu, Negative Surface Shielded Polymeric Micelles with Colloidal Stability for Intracellular Endosomal/Lysosomal Escape, Mol. Pharm. 15 (2018) 5374–5386.
[64] S. Honary, F. Zahir, Effect of zeta potential on the properties of nano-drug delivery systems - a review (Part 2), Trop. J. Pharm. Res. 12 (2013).
[65] E. Taipaleenmaki, S. Mouritzen, P. Schattling, Y. Zhang, B. Städler, Mucopenetrating Micelles with a PEG Corona, Nanoscale 9 (2017).
[66] S.P. Bandi, Y.S. Kumbhar, V.V.K. Venuganti, Effect of particle size and surface charge of nanoparticles in penetration through intestinal mucus barrier, J. Nanopart. Res. 22 (2020) 62.
[67] E. Taipaleenmäki, E. Brodszkij, B. Städler, Mucopenetrating Zwitterionic Micelles, ChemNanoMat 6 (2020) 744–750.
[68] Lecithin based nanoemulsions: A comparative study of the influence of non-ionic surfactants and the cationic phytosphingosine on physicochemical behaviour and skin permeation, Int. J. Pharm. 370 (2009) 181–186.
[69] T.T. Jubeh, Y. Barenholz, A. Rubinstein, Differential adhesion of normal and inflamed rat colonic mucosa by charged liposomes, Pharm. Res. 21 (2004) 447–453.
[70] P. Mi, H. Cabral, K. Kataoka, Ligand-installed nanocarriers toward precision therapy, Adv. Mater. 32 (2019) 1902604.
[71] Y. Wang, M.J. van Steenbergen, N. Beztsinna, Y. Shi, T. Lammers, C.F. van Nostrum, W.E. Hennink, Biotin-decorated all-HPMA polymeric micelles for paclitaxel delivery, J. Control. Release 328 (2020) 970–984.
[72] S. Zhong, D.J. Pochan, Cryogenic transmission electron microscopy for direct observation of polymer and small-molecule materials and structures in solution, Polym. Rev. 50 (2010) 287–320.
[73] N.P. Truong, M.R. Whittaker, C.W. Mak, T.P. Davis, The importance of nanoparticle shape in cancer drug delivery, Expert Opinion on Drug Delivery 12 (2015) 129–142.
[74] J. Kuntsche, J.C. Horst, H. Bunjes, Cryogenic transmission electron microscopy (cryo-TEM) for studying the morphology of colloidal drug delivery systems, Int. J. Pharm. 417 (2011) 120–137.
[75] D. Discher, Shape Effects of Filaments Versus Spherical Particles in Flow and Drug Delivery, 2008.
[76] D.A. Christian, S. Cai, O. Garbuzenko, T. Harada, A.L. Zajac, T. Minko, D. E. Discher, Flexible filaments for in vivo imaging and delivery: persistent circulation of filomicelles opens the dosage window for sustained tumor shrinkage, Mol. Pharm. 6 (2009) 1343–1352.
[77] N. Sancho Oltra, J. Swift, A. Mahmud, K. Rajagopal, S.M. Loverde, D.E. Discher, Filomicelles in nanomedicine – from flexible, fragmentable, and ligand-targetable drug carrier designs to combination therapy for brain tumors, J. Mater. Chem. B 1 (2013) 5177.
[78] N. Sancho Oltra, P. Nair, D.E. Discher, From stealthy polymersomes and filomicelles to self peptide-nanoparticles for cancer therapy, Ann. Revi. Chem. Biomol. Engi. 5 (2014) 281–299.
[79] W. Ke, N. Lu, A.A.-W.M.M. Japir, Q. Zhou, L. Xi, Y. Wang, D. Dutta, M. Zhou, Y. Pan, Z. Ge, Length effect of stimuli-responsive block copolymer prodrug filomicelles on drug delivery efficiency, J. Control. Release 318 (2020) 67–77.
[80] M. Imran, M.R. Shah, Shafiullah, Chapter 10 - Amphiphilic block copolymers–based micelles for drug delivery, in: A.M. Grumezescu (Ed.), Design and Development of New Nanocarriers, William Andrew Publishing, 2018, pp. 365–400.
[81] Z. Ahmad, A. Shah, M. Siddiq, H.-B. Kraatz, Polymeric micelles as drug delivery vehicles, RSC Adv. 4 (2014) 17028–17038.
[82] Y. Shi, T. Lammers, G. Storm, W.E. Hennink, Physico-chemical strategies to enhance stability and drug retention of polymeric micelles for tumor-targeted drug delivery, Macromol. Biosci. 17 (2017) 1600160.
[83] J. Lee, E.C. Cho, K. Cho, Incorporation and release behavior of hydrophobic drug in functionalized poly(d,l-lactide)-block–poly(ethylene oxide) micelles, J. Control. Release 94 (2004) 323–335.

[84] N. Phogat, M. Kohl, I. Uddin, A. Jahan, Chapter 11 - interaction of nanoparticles with biomolecules, protein, enzymes, and its applications, in: H.-P. Deigner, M. Kohl (Eds.), Precision Medicine, Academic Press, 2018, pp. 253–276.
[85] L. Zeng, J. Gao, Y. Liu, J. Gao, L. Yao, X. Yang, X. Liu, B. He, L. Hu, J. Shi, M. Song, G. Qu, G. Jiang, Role of protein corona in the biological effect of nanomaterials: Investigating methods, TrAC Trends Anal. Chem. 118 (2019) 303–314.
[86] E.Y. Chen, W.F. Liu, L. Megido, P. Díez, M. Fuentes, C. Fager, E. Olsson, I. Gessner, S. Mathur, Chapter 3 - Understanding and utilizing the biomolecule/nanosystems interface, in: V. Uskoković, D.P. Uskoković (Eds.), Nanotechnologies in Preventive and Regenerative Medicine, Elsevier, 2018, pp. 207–297.
[87] T.A. Diezi, Y. Bae, G.S. Kwon, Enhanced Stability of PEG-block-poly(N-hexyl stearate l-aspartamide) Micelles in the Presence of Serum Proteins, Mol. Pharm. 7 (2010) 1355–1360.
[88] Q. Zhou, L. Zhang, T. Yang, H. Wu, Stimuli-responsive polymeric micelles for drug delivery and cancer therapy 13, Int. J. Nanomedicine, 2018, pp. 2921–2942.
[89] L.C. Nelemans, L. Gurevich, Drug Delivery with polymeric nanocarriers-cellular uptake mechanisms, Materials (Basel, Switzerland) 13 (2020) 366.
[90] D. Maysinger, J. Lovrić, A. Eisenberg, R. Savić, Fate of micelles and quantum dots in cells, Eur. J. Pharm. Biopharm. 65 (2007) 270–281.
[91] T. Chen, B. He, J. Tao, Y. He, H. Deng, X. Wang, Y. Zheng, Application of Förster Resonance Energy Transfer (FRET) technique to elucidate intracellular and In Vivo biofate of nanomedicines, Adv. Drug Deliv. Rev. 143 (2019) 177–205.
[92] S.-Y. Lee, J.Y. Tyler, S. Kim, K. Park, J.-X. Cheng, FRET Imaging Reveals Different Cellular Entry Routes of Self-Assembled and Disulfide Bonded Polymeric Micelles, Mol. Pharm. 10 (2013) 3497–3506.
[93] C. Cui, Y.-N. Xue, M. Wu, Y. Zhang, P. Yu, L. Liu, R.-X. Zhuo, S.-W. Huang, Cellular uptake, intracellular trafficking, and antitumor efficacy of doxorubicin-loaded reduction-sensitive micelles, Biomaterials 34 (2013) 3858–3869.
[94] N. Rapoport, A. Marin, Y. Luo, G.D. Prestwich, M. Muniruzzaman, Intracellular uptake and trafficking of pluronic micelles in drug-sensitive and MDR cells: effect on the intracellular drug localization, J. Pharm. Sci. 91 (2002) 157–170.
[95] D.W. Miller, E.V. Batrakova, A.V. Kabanov, Inhibition of multidrug resistance-associated protein (MRP) functional activity with pluronic block copolymers, Pharm. Res. 16 (1999) 396–401.
[96] R.D. Dabholkar, R.M. Sawant, D.A. Mongayt, P.V. Devarajan, V.P. Torchilin, Polyethylene glycol–phosphatidylethanolamine conjugate (PEG–PE)-based mixed micelles: Some properties, loading with paclitaxel, and modulation of P-glycoprotein-mediated efflux, Int. J. Pharm. 315 (2006) 148–157.
[97] X. Jin, B. Zhou, L. Xue, W. San, Soluplus® micelles as a potential drug delivery system for reversal of resistant tumor, Biomed. Pharmacother. 69 (2015) 388–395.
[98] Y. Mu, Y. Fu, J. Li, X. Yu, Y. Li, Y. Wang, X. Wu, K. Zhang, M. Kong, C. Feng, X. Chen, Multifunctional quercetin conjugated chitosan nano-micelles with P-gp inhibition and permeation enhancement of anticancer drug, Carbohydr. Polym. 203 (2019) 10–18.
[99] S. Devi, V. Saini, M. Kumar, S. Bhatt, S. Gupta, A. Deep, A Novel Approach of Drug Localization through Development of Polymeric Micellar System Containing Azelastine HCl for Ocular Delivery, Pharm Nanotechnol. 7 (2019) 314–327.
[100] I.W. Hamley, Block Copolymers in Solution: Fundamentals and Applications, Wiley, 2005.
[101] M. Trujillo, M.P. Schramm, Measuring critical micelle concentration as a function of cavitand additives using surface tension and dye micellization, Ronald E McNair Postbac Achiev Program 14 (2010) 155–168.
[102] N. Scholz, T. Behnke, U. Resch-Genger, Determination of the critical micelle concentration of neutral and ionic surfactants with fluorometry, Conductometry, and Surface Tension—A Method Comparison, J. Fluoresc. 28 (2018) 465–476.
[103] T. Trimaille, K. Mondon, R. Gurny, M. Möller, Novel polymeric micelles for hydrophobic drug delivery based on biodegradable poly(hexyl-substituted lactides), Int. J. Pharm. 319 (2006) 147–154.
[104] X. Zhang, J.K. Jackson, H.M. Burt, Determination of surfactant critical micelle concentration by a novel fluorescence depolarization technique, J. Biochem. Biophys. Methods 31 (1996) 145–150.
[105] B. Jeong, Y. Han Bae, S. Wan Kim, Biodegradable thermosensitive micelles of PEG-PLGA-PEG triblock copolymers, Colloids Surf. B: Biointerfaces 16 (1999) 185–193.
[106] G. Basu Ray, S.P. Chakraborty, S.P. Moulik, Pyrene absorption can be a convenient method for probing critical micellar concentration (cmc) and indexing micellar polarity 294, J. Colloid Interface Sci., 2006, pp. 248–254.
[107] C.L. Zhao, M.A. Winnik, G. Riess, M.D. Croucher, Fluorescence probe techniques used to study micelle formation in water-soluble block copolymers, Langmuir 6 (1990) 514–516.
[108] Ö. Topel, B.A. Çakır, L. Budama, N. Hoda, Determination of critical micelle concentration of polybutadiene-block-poly(ethyleneoxide) diblock copolymer by fluorescence spectroscopy and dynamic light scattering, J. Mol. Liq. 177 (2013) 40–43.
[109] C. Rangel-Yagui, A. Pessoa, L. Tavares, Micellar solubilization of drugs, J. Pharm. Pharm. Sci. 8 (2005) 147–165.
[110] C. Rangel-Yagui, H. Hsu, A. Pessoa, L. Tavares, Micellar solubilization of ibuprofen - Influence of surfactant head groups on the extent of solubilization, Revista Brasileira De Ciencias Farmaceuticas - RBCF 41 (2005).
[111] A. Falamarzian, X.B. Xiong, H. Uludag, A. Lavasanifar, Polymeric micelles for siRNA delivery, J. Drug Deliv. Sci. Technol. 22 (2012) 43–54.
[112] A.M. Jhaveri, V.P. Torchilin, Multifunctional polymeric micelles for delivery of drugs and siRNA, Front. Pharmacol. 5 (2014) 77.
[113] Y. Shi, H. Zhu, Y. Ren, K. Li, B. Tian, J. Han, D. Feng, Preparation of protein-loaded PEG-PLA micelles and the effects of ultrasonication on particle size, Colloid Polym. Sci. 295 (2017) 259–266.
[114] S. Vauthey, M.E. Leser, N. Garti, H.J. Watzke, Solubilization of hydrophilic compounds in copolymer aggregates, J. Colloid Interface Sci. 225 (2000) 16–24.
[115] P.T. Wong, S.K. Choi, Mechanisms of drug release in nanotherapeutic delivery systems, Chem. Rev. 115 (2015) 3388–3432.
[116] D.F. de Andrade, C. Zuglianello, A.R. Pohlmann, S.S. Guterres, R.C.R. Beck, Assessing the in vitro drug release from lipid-core nanocapsules: a new strategy combining dialysis sac and a continuous-flow system, AAPS PharmSciTech 16 (2015) 1409–1417.
[117] S. D'Souza, A review of in vitro drug release test methods for nano-sized dosage forms, Adv. Pharm. 2014 (2014).
[118] D. Solomon, N. Gupta, N.S. Mulla, S. Shukla, Y.A. Guerrero, V. Gupta, Role of in vitro release methods in liposomal formulation development: challenges and regulatory perspective, AAPS J. 19 (2017) 1669–1681.
[119] V. Gupta, P. Trivedi, Chapter 15 - In vitro and in vivo characterization of pharmaceutical topical nanocarriers containing anticancer drugs for skin cancer treatment, in: A.M. Grumezescu (Ed.), Lipid Nanocarriers for Drug Targeting, William Andrew Publishing, 2018, pp. 563–627.
[120] Y. Zambito, E. Pedreschi, G. Di Colo, Is dialysis a reliable method for studying drug release from nanoparticulate systems?—A case study, Int. J. Pharm. 434 (2012) 28–34.
[121] S. Pescina, L.G. Lucca, P. Govoni, C. Padula, E.D. Favero, L. Cantù, P. Santi, S. Nicoli, Ex vivo conjunctival retention and transconjunctival transport of poorly soluble drugs using polymeric micelles, Pharmaceutics 11 (2019) 476.
[122] M. Yu, W. Yuan, D. Li, A. Schwendeman, S.P. Schwendeman, Predicting drug release kinetics from nanocarriers inside dialysis bags, J. Control. Release 315 (2019) 23–30.
[123] J.E. Yap, L. Zhang, J.T. Lovergrove, J.E. Beves, M.H. Stenzel, Visible light—responsive drug delivery nanoparticle via donor–acceptor stenhouse adducts (DASA), Macromol. Rapid Commun. 41 (2020) 2000236.
[124] T. Chen, B. He, J. Tao, Y. He, H. Deng, X. Wang, Y. Zheng, Application of forster resonance energy transfer (FRET) technique to elucidate intracellular and In Vivo biofate of nanomedicines, Adv. Drug Deliv. Rev. 143 (2019) 177–205.
[125] V. San Miguel, A.J. Limer, D.M. Haddleton, F. Catalina, C. Peinado, Biodegradable and thermoresponsive micelles of triblock copolymers based on 2-(N,N-dimethylamino)ethyl methacrylate and ε-caprolactone for controlled drug delivery, Eur. Polym. J. 44 (2008) 3853–3863.
[126] R. Tang, W. Ji, D. Panus, R.N. Palumbo, C. Wang, Block copolymer micelles with acid-labile ortho ester side-chains: synthesis, characterization, and enhanced drug delivery to human glioma cells, J. Control. Release 151 (2011) 18–27.
[127] J. Liu, F. Zeng, C. Allen, Influence of serum protein on polycarbonate-based copolymer micelles as a delivery system for a hydrophobic anti-cancer agent, J. Control. Release 103 (2005) 481–497.
[128] F. Jung, L. Nothnagel, F. Gao, M. Thurn, V. Vogel, M.G. Wacker, A comparison of two biorelevant in vitro drug release methods for nanotherapeutics based on advanced physiologically-based pharmacokinetic modelling, Eur. J. Pharm. Biopharm. 127 (2018) 462–470.
[129] P.M. van Hasselt, G.E.P.J. Janssens, T.K. Slot, M. van der Ham, T.C. Minderhoud, M. Talelli, L.M. Akkermans, C.J.F. Rijcken, C.F. van Nostrum, The influence of bile acids on the oral bioavailability of vitamin K encapsulated in polymeric micelles, J. Control. Release 133 (2009) 161–168.
[130] Y. Dai, X. Chen, X. Zhang, Recent advances in stimuli-responsive polymeric micelles via click chemistry, Polym. Chem. 10 (2019) 34–44.
[131] X. Gao, Z. Yu, B. Liu, J. Yang, X. Yang, Y. Yu, A smart drug delivery system responsive to pH/enzyme stimuli based on hydrophobic modified sodium alginate, Eur. Polym. J. 133 (2020) 109779.
[132] S. Kumar, J.-F. Allard, D. Morris, Y. Dory, M. Lepage, Y. Zhao, Near-infrared light sensitive polypeptide block copolymer micelles for drug delivery, J. Mater. Chem. 22 (15) (2012) 7252–7257.
[133] S. Bhattacharjee, DLS and zeta potential - What they are and what they are not? 235 J. Control. Release, 2016, pp. 337–351.
[134] B.J. Ree, J. Lee, Y. Satoh, K. Kwon, T. Isono, T. Satoh, M. Ree, A comparative study of dynamic light and x-ray scatterings on micelles of topological polymer amphiphiles, Polymers 10 (2018) 1347.
[135] J. Taillefer, M.C. Jones, N. Brasseur, J.E. van Lier, J.C. Leroux, Preparation and characterization of pH-responsive polymeric micelles for the delivery of photosensitizing anticancer drugs, J. Pharm. Sci. 89 (2000) 52–62.
[136] M.K. Gupta, T.A. Meyer, C.E. Nelson, C.L. Duvall, Poly(PS-b-DMA) micelles for reactive oxygen species triggered drug release, J. Control. Release 162 (2012) 591–598.
[137] M.A. Moretton, R.J. Glisoni, D.A. Chiappetta, A. Sosnik, Molecular implications in the nanoencapsulation of the anti-tuberculosis drug rifampicin within flower-like polymeric micelles, Colloids Surf. B: Biointerfaces 79 (2010) 467–479.
[138] S.M. Garg, M.R. Vakili, A. Lavasanifar, Polymeric micelles based on poly(ethylene oxide) and α-carbon substituted poly(ε-caprolactone): An in vitro study on the effect of core forming block on polymeric micellar stability, biocompatibility, and immunogenicity, Colloids Surf. B: Biointerfaces 132 (2015) 161–170.
[139] A.B. Ebrahim Attia, C. Yang, J.P.K. Tan, S. Gao, D.F. Williams, J.L. Hedrick, Y.-Y. Yang, The effect of kinetic stability on biodistribution and anti-tumor efficacy of drug-loaded biodegradable polymeric micelles, Biomaterials 34 (2013) 3132–3140.
[140] Y. Sun, Y. Liang, N. Hao, X. Fu, B. He, S. Han, J. Cao, Q. Ma, W. Xu, Y. Sun, Novel polymeric micelles as enzyme-sensitive nuclear-targeted dual-functional drug

delivery vehicles for enhanced 9-nitro-20(S)-camptothecin delivery and antitumor efficacy, Nanoscale 12 (2020) 5380–5396.
[141] J. Dong, Y. Wang, J. Zhang, X. Zhan, S. Zhu, H. Yang, G. Wang, Multiple stimuli-responsive polymeric micelles for controlled release, Soft Matter 9 (2013) 370–373.
[142] J.Z. Xu, S.H. Moon, B. Jeong, Y.S. Sohn, Thermosensitive micelles from PEGylated oligopeptides, Polymer 48 (2007) 3673–3678.
[143] C. Chang, H. Wei, J. Feng, Z.-C. Wang, X.-J. Wu, D.-Q. Wu, S.-X. Cheng, X.-Z. Zhang, R.-X. Zhuo, Temperature and pH Double Responsive Hybrid Cross-Linked Micelles Based on P(NIPAAm-co-MPMA)-b-P(DEA): RAFT Synthesis and "Schizophrenic" Micellization, Macromolecules 42 (2009) 4838–4844.
[144] H.B. Kern, S. Srinivasan, A.J. Convertine, D. Hockenbery, O.W. Press, P. S. Stayton, Enzyme-cleavable polymeric micelles for the intracellular delivery of proapoptotic peptides, Mol. Pharm. 14 (2017) 1450–1459.
[145] W.-H. Chen, G.-F. Luo, Q. Lei, H.-Z. Jia, S. Hong, Q.-R. Wang, R.-X. Zhuo, X.-Z. Zhang, MMP-2 responsive polymeric micelles for cancer-targeted intracellular drug delivery, Chem. Commun. 51 (2015) 465–468.
[146] Q. Yao, Z. Dai, J. Hoon Choi, D. Kim, L. Zhu, Building stable MMP2-responsive multifunctional polymeric micelles by an all-in-one polymer–lipid conjugate for tumor-targeted intracellular drug delivery, ACS Appl. Mater. Interfaces 9 (2017) 32520–32533.
[147] H. Shen, M. Zhou, Q. Zhang, A. Keller, Y. Shen, Zwitterionic light-responsive polymeric micelles for controlled drug delivery, Colloid Polym. Sci. 293 (2015) 1685–1694.
[148] J. Li, M. Huo, J. Wang, J. Zhou, J.M. Mohammad, Y. Zhang, Q. Zhu, A.Y. Waddad, Q. Zhang, Redox-sensitive micelles self-assembled from amphiphilic hyaluronic acid-deoxycholic acid conjugates for targeted intracellular delivery of paclitaxel, Biomaterials 33 (2012) 2310–2320.
[149] N. Jalili, K. Laxminarayana, A review of atomic force microscopy imaging systems: application to molecular metrology and biological sciences, Mechatronics 14 (2004) 907–945.
[150] M. Nasrollahzadeh, M. Atarod, M. Sajjadi, S.M. Sajadi, Z. Issaabadi, Chapter 6 - plant-mediated green synthesis of nanostructures: mechanisms, characterization, and applications, in: M. Nasrollahzadeh, S.M. Sajadi, M. Sajjadi, Z. Issaabadi, M. Atarod (Eds.), Interface Science and Technology, Elsevier, 2019, pp. 199–322.
[151] Y.L. Lyubchenko, Preparation of DNA and nucleoprotein samples for AFM imaging, Micron 42 (2011) 196–206.
[152] K. El Kirat, V. Burton Dupres, Y.F. Dupres, V. Fau Dufrene, Y.F. Dufrene, Sample preparation procedures for biological atomic force microscopy 218, J. Micros., 2005, pp. 199–207.
[153] J.A. Last, P. Russell, P.F. Nealey, C.J. Murphy, The applications of atomic force microscopy to vision science, Invest. Ophthalmol. Vis. Sci. 51 (2010) 6083–6094.
[154] C. Lamprecht, P. Hinterdorfer, A. Ebner, Applications of biosensing atomic force microscopy in monitoring drug and nanoparticle delivery, Expert Opin Drug Deliv 11 (2014) 1237–1253.
[155] Y. Lyubchenko, R. Shlyakhtenko, P. Harrington, S. Lindsay, Atomic force microscopy of long DNA: imaging in air and under water 90, Procl. Nat. Acad. Sci., 1993, pp. 2137–2140.
[156] H.G. Hansma, M. Bezanilla, F. Zenhausern, M. Adrian, R.L. Sinsheimer, Atomic force microscopy of DNA in aqueous solutions, Nucleic Acids Res. 21 (1993) 505–512.
[157] H. Kheiri Manjili, P. Ghasemi, H. Malvandi, M.S. Mousavi, E. Attari, H. Danafar, Pharmacokinetics and in vivo delivery of curcumin by copolymeric mPEG-PCL micelles, Eur. J. Pharm. Biopharm. 116 (2017) 17–30.
[158] E. Minatti, P. Viville, R. Borsali, M. Schappacher, A. Deffieux, R. Lazzaroni, Micellar morphological changes promoted by cyclization of PS-b-PI copolymer: DLS and AFM experiments, Macromolecules 36 (2003) 4125–4133.
[159] A. Schulz, S. Jaksch, R. Schubel, E. Wegener, Z. Di, Y. Han, A. Meister, J. Kressler, A.V. Kabanov, R. Luxenhofer, C.M. Papadakis, R. Jordan, Drug-induced morphology switch in drug delivery systems based on poly(2-oxazoline)s, ACS Nano 8 (2014) 2686–2696.
[160] F. Kohori, K. Sakai, T. Aoyagi, M. Yokoyama, Y. Sakurai, T. Okano, Preparation and characterization of thermally responsive block copolymer micelles comprising poly(N-isopropylacrylamide-b-DL-lactide), J. Control. Rel. 55 (1998) 87–98.
[161] J.K. Vasir, V. Labhasetwar, Quantification of the force of nanoparticle-cell membrane interactions and its influence on intracellular trafficking of nanoparticles, Biomaterials 29 (2008) 4244–4252.
[162] L. Xiao, X. Xiong, X. Sun, Y. Zhu, H. Yang, H. Chen, L. Gan, H. Xu, X. Yang, Role of cellular uptake in the reversal of multidrug resistance by PEG-b-PLA polymeric micelles, Biomaterials 32 (2011) 5148–5157.
[163] S.-E. Jin, J.W. Bae, S. Hong, Multiscale observation of biological interactions of nanocarriers: From nano to macro, Microsc. Res. Tech. 73 (2010) 813–823.
[164] J.L.S. Milne, M.J. Borgnia, A. Bartesaghi, E.E.H. Tran, L.A. Earl, D.M. Schauder, J. Lengyel, J. Pierson, A. Patwardhan, S. Subramaniam, Cryo-electron microscopy–a primer for the non-microscopist, FEBS J. 280 (2013) 28–45.
[165] T. Dokland, Back to the basics: The fundamentals of cryo-electron microscopy, Microsc. Microanal. 15 (2009) 1538.
[166] P.M. Frederik, D.H.W. Hubert, Cryoelectron microscopy of liposomes, in: Methods in Enzymology, Academic Press, 2005, pp. 431–448.
[167] K.S. Schmitz, Chapter 4 - Life Science, in: K.S. Schmitz (Ed.), Physical Chemistry, Elsevier, Boston, 2018, pp. 755–832.
[168] N.J. Severs, Freeze-fracture electron microscopy, Nat. Protoc. 2 (2007) 547–576.
[169] T. Li, C.J. Nowell, D. Cipolla, T. Rades, B.J. Boyd, Direct comparison of standard transmission electron microscopy and cryogenic-TEM in imaging nanocrystals inside liposomes, Mol. Pharm. 16 (2019) 1775–1781.
[170] A.C. Laan, A.G. Denkova, Cryogenic transmission electron microscopy: the technique of choice for the characterization of polymeric nanocarriers, EJNMMI Res. 7 (2017) 44.
[171] N. Petzetakis, A.P. Dove, R.K. O'Reilly, Cylindrical micelles from the living crystallization-driven self-assembly of poly(lactide)-containing block copolymers, Chem. Sci. 2 (2011) 955–960.
[172] P. Lim Soo, S.N. Sidorov, J. Mui, L.M. Bronstein, H. Vali, A. Eisenberg, D. Maysinger, Gold-labeled block copolymer micelles reveal gold aggregates at multiple subcellular sites, Langmuir 23 (2007) 4830–4836.
[173] O. Soga, C.F. van Nostrum, M. Fens, C.J.F. Rijcken, R.M. Schiffelers, G. Storm, W. E. Hennink, Thermosensitive and biodegradable polymeric micelles for paclitaxel delivery, J. Control. Release 103 (2005) 341–353.
[174] D. Velluto, D. Demurtas, J.A. Hubbell, PEG-b-PPS diblock copolymer aggregates for hydrophobic drug solubilization and release: cyclosporin a as an example, Mol. Pharm. 5 (2008) 632–642.
[175] C. Janas, Z. Mostaphaoui, L. Schmiederer, J. Bauer, M.G. Wacker, Novel polymeric micelles for drug delivery: Material characterization and formulation screening, Int. J. Pharm. 509 (2016) 197–207.
[176] N. Fairley, B. Hoang, C. Allen, Morphological control of poly(ethylene glycol)-block-poly(ε-caprolactone) copolymer aggregates in aqueous solution, Biomacromolecules 9 (2008) 2283–2291.
[177] C.J. Newcomb, T.J. Moyer, S.S. Lee, S.I. Stupp, Advances in cryogenic transmission electron microscopy for the characterization of dynamic self-assembling nanostructures, Curr. Opin. Colloid Interface Sci. 17 (2012) 350–359.
[178] S. Chavda, S. Yusa, M. Inoue, L. Abezgauz, E. Kesselman, D. Danino, P. Bahadur, Synthesis of stimuli responsive PEG47–b-PAA126–b-PSt32 triblock copolymer and its self-assembly in aqueous solutions, Eur. Polym. J. 49 (2013) 209–216.
[179] S.U. Egelhaaf, Kinetics of structural transitions in surfactant solutions, Curr. Opin. Colloid Interface Sci. 3 (1998) 608–613.
[180] H. Cui, T.K. Hodgdon, E.W. Kaler, L. Abezgauz, D. Danino, M. Lubovsky, Y. Talmon, D.J. Pochan, Elucidating the assembled structure of amphiphiles in solution via cryogenic transmission electron microscopy, Soft Matter 3 (2007) 945–955.
[181] N. Saito, Liu C. FauLodge, M.A. Lodge Tp Fau, M.A. Hillmyer, Multicompartment micelle morphology evolution in degradable miktoarm star terpolymers, ACS Nano., 2010, pp. 1907–1912.
[182] F.A. Plamper, J.R. McKee, A. Laukkanen, A. Nykänen, A. Walther, J. Ruokolainen, V. Aseyev, H. Tenhu, Miktoarm stars of poly(ethylene oxide) and poly (dimethylaminoethyl methacrylate): manipulation of micellization by temperature and light, Soft Matter 5 (2009) 1812–1821.
[183] Y. Yang, J. Dong, X. Li, Micelle to vesicle transitions of N-dodecyl-1, ω-diaminoalkanes: Effects of pH, temperature and salt, J. Colloid Interface Sci. 380 (2012) 83–89.
[184] K. Kuperkar, L. Abezgauz, D. Danino, G. Verma, P.A. Hassan, V.K. Aswal, D. Varade, P. Bahadur, Viscoelastic micellar water/CTAB/NaNO3 solutions: Rheology, SANS and cryo-TEM analysis, J. Colloid Interface Sci. 323 (2008) 403–409.
[185] T. Eshel-Green, H. Bianco-Peled, Mucoadhesive acrylated block copolymers micelles for the delivery of hydrophobic drugs, Colloids Surf. B: Biointerfaces 139 (2016) 42–51.
[186] E. Di Cola, I. Grillo, S. Ristori, Small angle x-ray and neutron scattering: powerful tools for studying the structure of drug-loaded liposomes, Pharmaceutics 8 (2016) 10.
[187] Y. Schilt, T. Berman, X. Wei, Y. Barenholz, U. Raviv, Using solution X-ray scattering to determine the high-resolution structure and morphology of PEGylated liposomal doxorubicin nanodrugs, Biochim. Biophys. Acta Gen. Subj. 1860 (2016) 108–119.
[188] Y.-D. Dong, B.J. Boyd, Applications of X-ray scattering in pharmaceutical science, Int. J. Pharm. 417 (2011) 101–111.
[189] Neutron, X-rays and light, Scattering Methods Applied to Soft Condensed Matter, 2008.
[190] T. Narayanan, Synchrotron small-angle X-ray scattering. In Soft Matter: Characterization, 2008.
[191] E.B. Manaia, M.P. Abuçafy, B.G. Chiari-Andréo, B.L. Silva, J.A. Oshiro Junior, L. A. Chiavacci, Physicochemical characterization of drug nanocarriers, Int. J. Nanomedicine 12 (2017) 4991–5011.
[192] J.P.A. Fairclough, I.W. Hamley, N.J. Terrill, X-ray scattering in polymers and micelles, Radiat. Phys. Chem. 56 (1999) 159–173.
[193] N.A.N. Hanafy, M. El-Kemary, S. Leporatti, Micelles structure development as a strategy to improve smart cancer therapy, Cancers 10 (2018) 238.
[194] J.S. Pedersen, Analysis of small-angle scattering data from colloids and polymer solutions: modeling and least-squares fitting, Adv. Colloid Interf. Sci. 70 (1997) 171–210.
[195] J. Pedersen, Form factors of block copolymer micelles with spherical, ellipsoidal and cylindrical cores, J. Appl. Crystall. 33 (2000) 637–640.
[196] J. Pedersen, Modelling of small-angle scattering date from colloids and polymer systems, neutrons, x-rays light scatt, Methods Appl. to Soft Condens. Matter (2002) 391–420.
[197] S. Kim, Y. Cho, J.H. Kim, S. Song, J. Lim, S.-H. Choi, K. Char, Structural analysis of bottlebrush block copolymer micelles using small-angle X-ray Scattering, ACS Macro Lett. 9 (2020) 1261–1266.
[198] I. Akiba, N. Terada, S. Hashida, K. Sakurai, T. Sato, K. Shiraishi, M. Yokoyama, H. Masunaga, H. Ogawa, K. Ito, N. Yagi, Encapsulation of a Hydrophobic Drug into a Polymer-Micelle Core Explored with Synchrotron SAXS, Langmuir 26 (2010) 7544–7551.

[199] C. Cao, J. Zhao, M. Lu, C.J. Garvey, M.H. Stenzel, Correlation between drug loading content and biological activity: the complexity demonstrated in paclitaxel-loaded glycopolymer micelle system, Biomacromolecules 20 (2019) 1545–1554.
[200] M. Szymusiak, J. Kalkowski, H. Luo, A.J. Donovan, P. Zhang, C. Liu, W. Shang, T. Irving, M. Herrera-Alonso, Y. Liu, Core–Shell Structure and Aggregation Number of Micelles Composed of Amphiphilic Block Copolymers and Amphiphilic Heterografted Polymer Brushes Determined by Small-Angle X-ray Scattering, ACS Macro Lett. 6 (2017) 1005–1012.
[201] K. Shiraishi, Y. Sanada, S. Mochizuki, K. Kawano, Y. Maitani, K. Sakurai, M. Yokoyama, Determination of polymeric micelles' structural characteristics, and effect of the characteristics on pharmacokinetic behaviors, J. Control. Release 203 (2015) 77–84.
[202] R. Klein, Interacting Colloidal Suspensions in Neutrons, X-Rays and Light, 2002.
[203] B. Fehér, K. Zhu, B. Nyström, I. Varga, J.S. Pedersen, Effect of temperature and ionic strength on micellar aggregates of oppositely charged thermoresponsive block copolymer polyelectrolytes, Langmuir 35 (2019) 13614–13623.
[204] A.L. Thompson, L.M. Mensah, B.J. Love, The effect of cisplatin on the nanoscale structure of aqueous PEO–PPO–PEO micelles of varying hydrophilicity observed using SAXS, Soft Matter 15 (2019) 3970–3977.
[205] J.B. Gilroy, P.A. Rupar, G.R. Whittell, L. Chabanne, N.J. Terrill, M.A. Winnik, I. Manners, R.M. Richardson, Probing the structure of the crystalline core of field-aligned, monodisperse, cylindrical polyisoprene-block-polyferrocenylsilane micelles in solution using synchrotron small- and wide-angle X-ray scattering, J. Am. Chem. Soc. 133 (2011) 17056–17062.
[206] D.W. Hayward, D.J. Lunn, A. Seddon, J.R. Finnegan, O.E.C. Gould, O. Magdysyuk, I. Manners, G.R. Whittell, R.M. Richardson, Structure of the crystalline core of fiber-like polythiophene block copolymer micelles, Macromolecules 51 (2018) 3097–3106.
[207] O. Lieleg, K. Ribbeck, Biological hydrogels as selective diffusion barriers, Trends Cell Biol. 21 (2011) 543–551.
[208] Q. Xu, L.M. Ensign, N.J. Boylan, A. Schön, X. Gong, J.-C. Yang, N.W. Lamb, S. Cai, T. Yu, E. Freire, J. Hanes, Impact of surface polyethylene glycol (PEG) density on biodegradable nanoparticle transport in mucus ex vivo and distribution in vivo, ACS Nano 9 (2015) 9217–9227.
[209] G. Prosperi-Porta, S. Kedzior, B. Muirhead, H. Sheardown, Phenylboronic-acid-based polymeric micelles for mucoadhesive anterior segment ocular drug delivery, Biomacromolecules 17 (2016) 1449–1457.
[210] M.A. Safwat, H.F. Mansour, A.K. Hussein, S. Abdelwahab, G.M. Soliman, Polymeric micelles for the ocular delivery of triamcinolone acetonide: preparation and in vivo evaluation in a rabbit ocular inflammatory model, Drug Delivery 27 (2020) 1115–1124.
[211] S.B.D.S. Ferreira, G. Braga, É.L. Oliveira, J.B. da Silva, H.C. Rosseto, L.V. de Castro Hoshino, M.L. Baesso, W. Caetano, C. Murdoch, H.E. Colley, M.L. Bruschi, Design of a nanostructured mucoadhesive system containing curcumin for buccal application: from physicochemical to biological aspects, Beilstein J. Nanotechnol. 10 (2019) 2304–2328.
[212] A. Clementino, M. Batger, G. Garrastazu, M. Pozzoli, E. Del Favero, V. Rondelli, B. Gutfilen, T. Barboza, M.B. Sukkar, S.A.L. Souza, L. Cantù, F. Sonvico, The nasal delivery of nanoencapsulated statins - an approach for brain delivery, Int. J. Nanomedicine 11 (2016) 6575–6590.
[213] E. Di Cola, L. Cantu, P. Brocca, V. Rondelli, G.C. Fadda, E. Canelli, P. Martelli, A. Clementino, F. Sonvico, R. Bettini, E. Del Favero, Novel O/W nanoemulsions for nasal administration: Structural hints in the selection of performing vehicles with enhanced mucopenetration, Colloids Surf. B: Biointerfaces 183 (2019) 110439.
[214] T. Narayanan, O. Konovalov, Synchrotron scattering methods for nanomaterials and soft matter research, Materials (Basel, Switzerland) 13 (2020) 752.
[215] J. Kalkowski, C. Liu, P. Leon-Plata, M. Szymusiak, P. Zhang, T. Irving, W. Shang, O. Bilsel, Y. Liu, In situ measurements of polymer micellization kinetics with millisecond temporal resolution, Macromolecules 52 (2019) 3151–3157.
[216] R. Takahashi, T. Narayanan, S.-i. Yusa, T. Sato, Kinetics of morphological transition between cylindrical and spherical micelles in a mixture of anionic–neutral and cationic–neutral block copolymers studied by time-resolved SAXS and USAXS, Macromolecules 51 (2018) 3654–3662.
[217] J.I. Hare, T. Lammers, M.B. Ashford, S. Puri, G. Storm, S.T. Barry, Challenges and strategies in anti-cancer nanomedicine development: An industry perspective, Adv. Drug Deliv. Rev. 108 (2017) 25–38.
[218] S. Kunjachan, J. Ehling, G. Storm, F. Kiessling, T. Lammers, Noninvasive imaging of nanomedicines and nanotheranostics: principles, progress, and prospects, Chem. Rev. 115 (2015) 10907–10937.
[219] H. Suzuki, Y.H. Bae, Evaluation of drug penetration with cationic micelles and their penetration mechanism using an in vitro tumor model, Biomaterials 98 (2016) 120–130.
[220] M.C. Valerii, M. Benaglia, C. Caggiano, A. Papi, A. Strillacci, G. Lazzarini, M. Campieri, P. Gionchetti, F. Rizzello, E. Spisni, Drug delivery by polymeric micelles: an in vitro and in vivo study to deliver lipophilic substances to colonocytes and selectively target inflamed colon, Nanomedicine 9 (2013) 675–685.
[221] X. Dai, Z. Yue, M.E. Eccleston, J. Swartling, N.K.H. Slater, C.F. Kaminski, Fluorescence intensity and lifetime imaging of free and micellar-encapsulated doxorubicin in living cells, Nanomedicine 4 (2008) 49–56.
[222] P.A. Ma, S. Liu, Y. Huang, X. Chen, L. Zhang, X. Jing, Lactose mediated liver-targeting effect observed by ex vivo imaging technology, Biomaterials 31 (2010) 2646–2654.
[223] D.-Q. Wu, B. Lu, C. Chang, C.-S. Chen, T. Wang, Y.-Y. Zhang, S.-X. Cheng, X.-J. Jiang, X.-Z. Zhang, R.-X. Zhuo, Galactosylated fluorescent labeled micelles as a liver targeting drug carrier, Biomaterials 30 (2009) 1363–1371.
[224] Y. Shi, S. Kunjachan, Z. Wu, F. Gremse, D. Moeckel, M. van Zandvoort, F. Kiessling, G. Storm, C.F. van Nostrum, W.E. Hennink, T. Lammers, Fluorophore labeling of core-crosslinked polymeric micelles for multimodal in vivo and ex vivo optical imaging, Nanomedicine 10 (2015) 1111–1125.
[225] M. Liu, J. Fu, J. Li, L. Wang, Q. Tan, X. Ren, Z. Peng, H. Zeng, Preparation of tri-block copolymer micelles loading novel organoselenium anticancer drug BBSKE and study of tissue distribution of copolymer micelles by imaging in vivo method, Int. J. Pharm. 391 (2010) 292–304.
[226] H. He, L. Wang, Y. Ma, Y. Yang, Y. Lv, Z. Zhang, J. Qi, X. Dong, W. Zhao, Y. Lu, W. Wu, The biological fate of orally administered mPEG-PDLLA polymeric micelles, J. Control. Release 327 (2020) 725–736.
[227] Y. Ma, H. He, W. Fan, Y. Li, W. Zhang, W. Zhao, J. Qi, Y. Lu, X. Dong, W. Wu, In vivo fate of biomimetic mixed micelles as nanocarriers for bioavailability enhancement of lipid–drug conjugates, ACS Biomater. Sci. Eng. 3 (2017) 2399–2409.
[228] F. Hsiao, P.-Y. Huang, T. Aoyagi, S.-F. Chang, J. Liaw, In vitro and in vivo assessment of delivery of hydrophobic molecules and plasmid DNAs with PEO–PPO–PEO polymeric micelles on cornea, J. Food Drug Anal. 26 (2017).
[229] R.B. Sekar, A. Periasamy, Fluorescence resonance energy transfer (FRET) microscopy imaging of live cell protein localizations, J. Cell Biol. 160 (2003) 629–633.
[230] S.W. Morton, X. Zhao, M.A. Quadir, P.T. Hammond, FRET-enabled biological characterization of polymeric micelles, Biomaterials 35 (2014) 3489–3496.
[231] S.J. Leavesley, T.C. Rich, Overcoming limitations of FRET measurements, Cytometry. Part A 89 (2016) 325–327.
[232] S. Jiwpanich, J.-H. Ryu, S. Bickerton, S. Thayumanavan, Noncovalent Encapsulation Stabilities in Supramolecular Nanoassemblies, J. Am. Chem. Soc. 132 (2010) 10683–10685.
[233] J. Lu, S.C. Owen, M.S. Shoichet, Stability of Self-Assembled Polymeric Micelles in Serum, Macromolecules 44 (2011) 6002–6008.
[234] H. Chen, S. Kim, L. Li, S. Wang, K. Park, J.-X. Cheng, Release of hydrophobic molecules from polymer micelles into cell membranes revealed by Förster resonance energy transfer imaging, Proc. Natl. Acad. Sci. 105 (2008) 6596.
[235] H. Chen, W. Kim, S. Fau, H. He, Fast release of lipophilic agents from circulating PEG-PDLLA micelles revealed by in vivo forster resonance energy transfer imaging 24, Langmuir, 2008, pp. 5213–5217.
[236] X. Sun, G. Wang, H. Zhang, S. Hu, X. Liu, J. Tang, Y. Shen, The blood clearance kinetics and pathway of polymeric micelles in cancer drug delivery, ACS Nano 12 (2018) 6179–6192.
[237] H. Zhang, H. Li, Z. Cao, J. Du, L. Yan, J. Wang, Investigation of the in vivo integrity of polymeric micelles via large Stokes shift fluorophore-based FRET, J. Control. Release 324 (2020) 47–54.
[238] M. Watanabe, K. Kawano, M. Yokoyama, P. Opanasopit, T. Okano, Y. Maitani, Preparation of camptothecin-loaded polymeric micelles and evaluation of their incorporation and circulation stability, Int. J. Pharm. 308 (2006) 183–189.
[239] J. Liu, F. Zeng, C. Allen, In vivo fate of unimers and micelles of a poly(ethylene glycol)-block-poly(caprolactone) copolymer in mice following intravenous administration, Eur. J. Pharm. Biopharm. 65 (2007) 309–319.
[240] M. Wagner, S. Holzschuh, A. Traeger, A. Fahr, U.S. Schubert, Asymmetric flow field-flow fractionation in the field of nanomedicine, Anal. Chem. 86 (2014) 5201–5210.
[241] Y. Hu, R.M. Crist, J.D. Clogston, The utility of asymmetric flow field-flow fractionation for preclinical characterization of nanomedicines, Anal. Bioanal. Chem. 412 (2020) 425–438.
[242] Y. Liu, M.H.A.M. Fens, R.B. Capomaccio, D. Mehn, L. Scrivano, R.J. Kok, S. Oliveira, W.E. Hennink, C.F. van Nostrum, Correlation between in vitro stability and pharmacokinetics of poly(ε-caprolactone)-based micelles loaded with a photosensitizer, J. Control. Release 328 (2020) 942–951.
[243] T.D. Langridge, R.A. Gemeinhart, Toward understanding polymer micelle stability: Density ultracentrifugation offers insight into polymer micelle stability in human fluids, J. Control. Release 319 (2020) 157–167.
[244] J.A. Garner, ORGANELLES | Centrifugation, in: I.D. Wilson (Ed.), Encyclopedia of Separation Science, Academic Press, Oxford, 2000, pp. 3586–3596.
[245] L.L. Bondoc, Viruses: Centrifugation, in: I.D. Wilson (Ed.), Encyclopedia of Separation Science, Academic Press, Oxford, 2000, pp. 4433–4436.
[246] E. Rødahl, Ultracentrifugation, in: P.J. Delves (Ed.), Encyclopedia of Immunology (Second Edition), Elsevier, Oxford, 1998, pp. 2446–2448.
[247] P. Li, A. Kumar, J. Ma, Y. Kuang, L. Luo, X. Sun, Density gradient ultracentrifugation for colloidal nanostructures separation and investigation, Sci. Bull. 63 (2018) 645–662.
[248] Regulatory aspects on nanomedicines, Biochem. Biophys. Res. Commun. 468 (2015) 504–510.
[249] Y.H. Choi, H.-K. Han, Nanomedicines: current status and future perspectives in aspect of drug delivery and pharmacokinetics 48, 2018, p. 60.
[250] M. Bagheri, M.H. Fens, T.G. Kleijn, R.B. Capomaccio, D. Mehn, P.M. Krawczyk, E. M. Scutigliani, A. Gurinov, M. Baldus, N.C.H. van Kronenburg, R.J. Kok, M. Heger, C.F. van Nostrum, W.E. Hennink, In vitro and in vivo studies on hpma-based polymeric micelles loaded with curcumin, Mol. Pharm. 18 (3) (2021) 1247–1263.
[251] G.S. Kwon, S.R. Croy, Polymeric micelles for drug delivery, Curr. Pharm. Des. 12 (2006) 4669–4684.